Chem. Rev. **2005,** *105,* 3889−3910

The Magnetic Shielding Function of Molecules and Pi-Electron Delocalization

Thomas Heine,† Clémence Corminboeuf,‡,§ and Gotthard Seifert*,†

Institut für Physikalische Chemie und Elektrochemie, TU-Dresden, D-01062 Dresden, Germany, Département de Chimie Physique, Université de Genève, CH-1211 Genève, Switzerland, and Department of Chemistry and Center for Computational Chemistry, University of Georgia, Athens, Georgia 30602

Received December 1, 2004

Contents

1. Introduction 3889
2. Interaction of Molecules with Magnetic Fields: The Shielding Function 3892
3. Special NMR Properties of Aromatic Molecules 3894
4. Magnetically Induced Current Densities and Related Models 3897
5. Shielding Functions and IMFs of Molecules 3901
6. Electron Delocalization and Magnetic Response of Example Molecules: Benzene, Cyclobutadiene, and Al_4^{n-} 3905
7. Conclusions 3908
8. Acknowledgments 3908
9. References 3908

1. Introduction

Measurement and theoretical prediction of magnetic properties have become an essential tool for the chemical community. Today, NMR spectroscopy is probably the most powerful of all analytical techniques used routinely in chemistry and biochemistry. It has now been about 60 years since the phenomenon was first observed experimentally and since the theory for magnetic shielding of nuclei in molecules was developed. Quantum chemical shielding tensor calculations can nowadays be performed with a very high accuracy and are routinely used to predict the NMR resonance lines of molecules.

The energy levels studied in NMR spectroscopy are the spin eigenstates of chemically bonded nuclei in the presence of an external magnetic field. The nuclear magnetic moment of an NMR active nucleus can align with an externally applied magnetic field of strength $\vec{B}_{\rm ext}$ in only $2I + 1$ ways, either reinforcing or opposing $\vec{B}_{\rm ext}$. The precise resonant frequencies are associated with transitions between these different energy levels, which depend on the effective magnetic field at the nucleus. The effective magnetic field is the superposition of the external magnetic field $\vec{B}_{\rm ext}$ and that of the field induced by the electrons of the molecule itself, $\vec{B}_{\rm ind}$, at the position of the nucleus. The induced field, and hence the shielding tensor at the nucleus $\vec{\sigma}$, is characteristic for the electron distribution, and hence the structure, of the molecule. This makes NMR such a powerful analytical tool.

Experimentally, the nuclear magnetic shielding tensor is—so far—inaccessible, but the chemical shift tensor, $\vec{\delta}$, which is the difference of the shielding tensor with respect to that of a reference compound, is obtained at the position of the nuclei. The theory of the nuclear magnetic shielding was outlined originally by Ramsey.[1] Within this formalism, the energy of a molecule in the presence of an external magnetic field, $\vec{B}_{\rm ext}$, and of a nucleus with a magnetic moment, $\vec{\mu}$, can be expressed in a Taylor series expansion with respect to $\vec{B}_{\rm ext}$ and $\vec{\mu}$. The components of the shielding tensor $\sigma_{\alpha\beta}$ are hence the bilinear second-order expansion coefficients in this series, defined as the second derivatives of the total energy of the system, E, with respect to the external magnetic field, $\vec{B}_{\rm ext}$, and the magnetic moment of the nucleus $\vec{\mu}$:

$$\sigma_{\alpha\beta} = \frac{\partial^2 E}{\partial(\vec{B}_{\rm ext})_\alpha\, \partial(\vec{\mu})_\beta} \tag{1.1}$$

Ramsey applied straightforward perturbation theory to derive explicit expressions for the shielding tensor. As it will be shown below, these expressions may be written also in terms of classical electrodynamics as the interaction between the magnetic moment $\vec{\mu}$ and the current density $\vec{j}(\vec{r})$, induced by the external magnetic field as given in Biot−Savart's law. The induced magnetic field (IMF) can be calculated from Biot−Savart's law at any point in space, independent of the presence of a nucleus. This allows one to introduce a tensorial shielding function, $\vec{\vec{\sigma}}(\vec{r})$. The magnetic shielding function can be pictorially understood: The external field $\vec{B}_{\rm ext}$ creates a current density in the molecule. This current density induces another magnetic field. This induced field "shields" the external field, and in NMR experiment, the nuclei experience a field, different from $\vec{B}_{\rm ext}$ by the induced field, following the relation

$$(\vec{B}_{\rm ind})_\alpha = -\sum_{\beta=1}^{3} \sigma_{\alpha\beta}\, (\vec{B}_{\rm ext})_\beta \tag{1.2}$$

Beside the induced current density, this magnetic shielding function will be the central quantity discussed in this review, as most approaches treating electron delocalization in terms of magnetic properties relate directly to either of these two functions in space.

The history of quantitative shielding calculations is not as long as one might expect from the date of

---

† Institut für Physikalische Chemie und Elektrochemie.
‡ Université de Genève.
§ University of Georgia.

10.1021/cr030082k CCC: \$53.50

Thomas Heine was born in Seehausen (Germany) in 1970. He studied physics at TH Merseburg and TU Clausthal (Germany) and received his Master's Degree at the Institute of Theoretical Physics in 1995, under the supervision of Prof. Lothar Fritsche. During his time as a Ph.D. student (1995–1999) at TU Dresden (Germany), Institute of Theoretical Physics, supervised by Prof. Gotthard Seifert, he worked as visiting researcher at the Department of Chemistry, University of Montreal (Canada), in the group of Prof. Dennis Salahub and at the School of Chemistry, Exeter University (United Kingdom), in the group of Prof. Patrick Fowler. After postdoctoral stages at the Department of Chemistry, University of Bologna (Italy), working with Prof. Francesco Zerbetto, and the Department of Physical Chemistry, University of Geneva (Switzerland), in the group of Prof. Jacques Weber, he joined the Institute of Physical Chemistry and Electrochemistry of TU Dresden in 2002. His research interests are the development of methods of theoretical chemistry, including density functional theory and tight-binding methods, and their applications, in particular to study magnetic properties of molecules and solids.

Clémence Corminboeuf studied Chemistry at the University of Geneva. After graduating in 2000, she carried out her Masters research in theoretical chemistry at the National Research Council in Ottawa, Canada, with Prof. D. R. Salahub. She completed her Ph.D. in Quantum Chemistry in 2004 at the University of Geneva together with Prof. J. Weber and Dr. T. Heine in TU-Dresden. The majority of her research has been devoted to investigations of electronic delocalization in annulenes and inorganic clusters. Since 2001, she has collaborated with Prof. P. v. R. Schleyer at the University of Georgia, where she occupied a postdoctoral position in 2004. She is presently at New York University under a NSF research grant.

Gotthard Seifert studied Chemistry at the TU Dresden, where he received his diploma in 1975 and graduated also to a Dr. rer. nat. (Ph.D.) in 1979. From 1979 to 1992, he worked as a research assistant at the Institute of Theoretical Physics at the TU Dresden. In 1988, he received his habilitation in theoretical physics. In 1989 and 1990, he worked as a visiting scientist and visiting professor at the International School for Advanced Studies (SISSA) in Trieste and at the EPFL. In 1991, he was a visiting scientist at the Forschungszentrum in Jülich. From 1992 to 1998, he was again at the Institute of Theoretical Physics at the TU Dresden as a lecturer/professor. In 1998, he moved to the Universität Paderborn (Theoretical Physics). In 2001, he became a professor of Physical Chemistry at the TU Dresden. His research interests are in the areas of quantum chemistry, cluster physics and chemistry, and computational materials research.

the rigorous formulation of the theory in 1950.[1] The most significant progress has indeed been achieved during the past decade (for a recent overview, see ref 2). There are a number of difficulties with magnetic properties that prevented early success of quantum−chemical techniques. An example is the well-known gauge−origin problem, which limited the applicability and accuracy of the pioneering computations of Lipscomb.[3] The establishment of practical and efficient solutions for the gauge problem caused the breakthrough in the field of NMR chemical shift calculations.

For instance, the gauge-including atomic orbitals (in the original work called gauge-invariant atomic orbitals, GIAOs) suggested by London[4] depend explicitly on the magnetic field. They were first used for semiempirical computations by Hameka[5] and Pople[6] and later by Ditchfield[7] to calculate NMR shielding tensors from ab initio molecular orbital wave functions. Since then, Häser et al.[8] and Wolinski and Pulay[9] improved the efficiency of the GIAO approach and demonstrated that modern analytical derivative theory[10] can be efficiently used for the calculation of the magnetic shielding, making the method practical for large molecules.[8,11] The GIAO approach has been extended by Jørgensen and coworkers to include multiconfigurational self-consistent field interactions for calculations of NMR shielding tensors.[12,13] The method has been generalized to include various post-Hartree−Fock (HF) treatments of electron correlation[14] including many-body perturbation theory[14,15] and coupled cluster theory.[16] A recent review of Gauss and Stanton is strongly recommended.[17] One of the most popular alternatives to the GIAO method is the mathematically and computationally less demanding "individual gauge for localized orbitals" (IGLO) method, preluded by the pioneering work of Staemmler[18] and first formulated in a rigorous way by Kutzelnigg.[19] The IGLO method allowed the first ab initio NMR computations for larger systems and, hence, initiated this rather recent field of quantum chemistry.[20−22] A further, related, alternative to treat the gauge problem is the localized orbital/local origin (LORG) approach of Hansen and Bouman.[23] The IGLO and LORG methods express the shielding tensor in terms of localized molecular orbitals (LMOs) and choose an individual gauge origin for each LMO. Another choice of distributed gauge origin has been suggested by Bader and Keith. They introduced the individual gauges for atoms in molecules[24] and continuous set of gauge transformations (CSGT)[25] methods, the latter one denoted continuous transformation of the origin of the current density (CTOCD) by Lazzeretti, Malagoli, and Zanasi.[26]

The computation of magnetic properties using density functional theory (DFT) meets fundamental limitations within the formulation of the theory by Hohenberg, Kohn, and Sham.[27,28] The Hohenberg–Kohn theorem has been extended to the fully relativistic case, including the external magnetic field, by Rajagopal and Callaway.[29,30] Eschrig, Seifert, and Ziesche formulated Kohn–Sham-like equations, which explicitly include the magnetic field,[31] and the application of this approach to calculations of nuclear magnetic shielding in molecules was demonstrated.[32–35] So far, no reasonable exchange correlation (XC) current density functional has been proposed yet and computations have been limited to an uncoupled perturbation theory within DFT. The application of uncoupled DFT for the computation of NMR chemical shifts has been rather successful,[2,36–38] but for heavier nuclei, some limitations apply.[39] The work on current density-dependent XC functionals has been continued[40–49] but without coming up with an applicable solution. The theoretical framework of DFT for the computation of the magnetic shielding will be revisited in the next section. Despite the remarkable success of DFT in various domains in the early nineties, valuable DFT implementations of the NMR shielding tensor are quite recent. The earliest attempts (see, for example, ref 35) do not address the gauge problem at all. Accordingly, the results were unreliable. Friedrich et al.[33,34] were the first to combine the GIAO method[4,7] with DFT, but their implementation was restricted by the use of the Xα approximation[32–34,50,51] for the XC energy functional and to minimal basis sets. In the early 1990s, Malkin and co-workers published a series of pioneering papers on the calculation of NMR properties, including shieldings, within DFT.[36,52–54] In their implementation, they combine modern DFT with the IGLO method.[18–20] Furthermore, they introduced somewhat ad hoc a correction term to simulate the current dependency of the XC functional and thus improved the agreement of the calculated shieldings with experimental results.[36,38] More recent implementations of the GIAO technique within the DFT formalism have been subsequently proposed by Schreckenbach[37] and Cheeseman.[55]

In this article, we discuss the magnetic shielding as a function in space, the shielding function. Already in 1958, Johnson and Bovey discussed the isotropic shielding as a function of the position within a coordinate system centered at the molecule.[56] The same quantity has been entitled differently in the following decades, and a manifold of methods have been established, which are directly related to the shielding function. The tensorial magnetic shielding function is given as a Cartesian tensor at any point in space. Usually, the coordinate system of the molecule in standard orientation is chosen. The same quantity has been called—in a somewhat misleading way—nuclear magnetic shielding density by Jameson and Buckingham.[57,58] Later, Hansen and his group used the term molecular magnetic shielding field.[59] The isotropic values of the tensorial magnetic shielding function can be discussed by its values in space or by isoshielding surfaces and lines. Also, they have been introduced in the pioneering work of Johnson and Bovey as early as 1958.[56] Nowadays, it is most common to compute the negative isotropic magnetic shielding function at selected positions in space. This has been called nucleus-independent chemical shift (NICS) by Schleyer and his group[60] and is today the most commonly applied probe of aromaticity,[61] for example. It was also Schleyer and his group who suggested that the shielding function, or rather NICS, should be computed at several positions in and around the molecule—so-called NICS grids—to gain a better understanding of the degree of (local) “aromaticity” of the studied molecule.[62–64] Wolinski used the terms shielding surface and neutron chemical shifts for the isotropic shielding function in molecules,[65] while Klod and Kleinpeter called the isosurface of the same quantity isochemical shielding surface (ICSS).[66] People had quite different motivation to compute the shielding function at points different from the nuclei: Already in the original work, where a semiempirical shielding function was used to access ^{1}H NMR chemical shifts with great precision,[56] the shielding function around the benzene molecule was computed for “curiosity”. Later, the shielding function was investigated to gain more information on the electronic structure of a molecule[57,58,65] and to have a probe of aromaticity.[59,60,62,66]

This review interprets the approaches that are used in the literature to discuss electron delocalization and aromaticity in terms of magnetic shieldings and current densities. It is structured as follows: In section 2, the basic theory for the computation of the tensorial magnetic shielding function of a molecule is reviewed. It will be shown that the shielding function in a molecule can be computed at any position in space and that at positions of the nuclei the shielding function is identical to NMR chemical shielding tensors. Special emphasis is given to the computation of the shielding function using DFT, on which most of the applications discussed in this review are based. Readers less interested in the theoretical background might eventually skip section 2. In section 3, the special magnetic properties of aromatic molecules are discussed, both in terms of the ring current model and in terms of electron delocalization. The special role of electron delocalization of π-systems of carbon structures is discussed from the viewpoint of the establishment of semiempirical methods and in terms of various applications on carbon structures. In the fourth section, we discuss several models, which are related to the current density, namely, the mapping of the current density in several approaches, the topological analysis of the current density, the anisotropy of the current (induced) density (ACID) approach, and the aromatic ring current shielding (ARCS) method. The fifth section deals with methods that are directly related to the computation of the magnetic shielding function in and around molecules. We will show that a number of approaches are equivalent with the computation of the magnetic shielding function, as either a tensor or their isotropic value. As these approaches have been developed to suit different purposes, a unification of the terminology will be helpful for the general chemical community. The IMF can be computed directly from the shielding function and is also reviewed in section 5. Finally, in section 6, we compare the results of most of the methods discussed in this review on four illustrative molecules: The aromatic standard, benzene; the antiaromatic standard, D_{2h} cyclobutadiene; and the Al_4^{2-} and Al_4^{4-} clusters, which led to controversial interpretations of aromaticity in the recent literature.

2. Interaction of Molecules with Magnetic Fields: The Shielding Function

Numerous methods for the calculation of magnetic shielding tensors in molecules have been developed since the fundamental formulation of the theory for nuclear magnetic shielding by Ramsey.[1] Most of these methods are based on HF perturbation theory. LCAO "ab initio" calculations with large basis sets have been performed within the coupled HF (CHF) perturbation theory for quite a long time (see, for example, ref 3). A great progress has been achieved by the use of proper gauge transformations, in particular in the CHF calculations.[7] Simplified variants of the CHF scheme were used by several authors.[67−70] Especially, the uncoupled HF perturbation theory has been applied widely in the past (see, for example, refs 67 and 68). Finally, the methods of gauge transformations brought also remarkable success in the calculations of shielding constants also of larger molecules.[19−22]

Several reviews on calculations of NMR shielding tensors have been published—see, for example, refs 2, 61, 71, and 72. Because, in principle, these methods are all applicable to calculate the magnetic shielding function of diamagnetic molecules, a short review of the derivation of the basic theory will be given here. (Conventions in this section are as follows: k denotes indices of nuclei, j denotes orbital indices, arrows denote vectors, and stacked arrows denote matrices and two-dimensional tensors. Lower indices give the order of the wave function, while upper indices in parentheses denote the perturbation order in $\vec{B}$.) The current density $\vec{j}(\vec{r})$ of a diamagnetic molecule in a stationary external magnetic field $\vec{B}_{\text{ext}}$ in the electronic ground state with the corresponding wave function Ψ_0 is given by:

$$\vec{j}(\vec{r}) = \frac{i}{2}\,[(\vec{\nabla}\Psi_0^*)\Psi_0 - \Psi_0^*(\vec{\nabla}\Psi_0)] - \frac{1}{c}\vec{A}\Psi_0^*\Psi_0 \quad (2.1)$$

where $\vec{A}$ is the vector potential of the external magnetic field. The induced field $\vec{B}_{\text{ind}}$ at any point $\vec{r}_{\text{k}}$ of a molecule in an external magnetic field $\vec{B}_{\text{ext}}$ can be calculated using Biot−Savart's law:

$$\vec{B}_{\text{ind}}(\vec{r}_{\text{k}}) = \frac{1}{c}\int \frac{\vec{j}(\vec{r}) \times \vec{r}_{\text{k}}}{r_{\text{k}}^3}\,\mathrm{d}^3r \quad (2.2)$$

Alternatively to the induced field, a tensorial shielding function $\vec{\vec{\sigma}}(\vec{r}_{\text{k}})$ ($\vec{\vec{\sigma}} \leftrightarrow \sigma_{\alpha\beta}$) may be introduced to describe the response of the electronic system in a molecule to the external magnetic field:

$$(\vec{B}_{\text{ind}})_\alpha = -\sum_{\beta=1}^{3} \sigma_{\alpha\beta}\,(\vec{B}_{\text{ext}})_\beta \quad (2.3)$$

This shielding function is just the generalization of the shielding tensor in NMR spectroscopy, where the induced field, respectively, the shielding field, is needed only at a few specific points in space, namely, at the positions of the nuclei.

For the calculation of the induced field via Biot−Savart's law, the current density $\vec{j}$ has to be calculated from the wave function Ψ_0 under consideration of the external magnetic field. The Hamiltonian for a diamagnetic molecule with N electrons in a stationary external magnetic field ($\vec{B}_{\text{ext}}$) has the following form:

$$\hat{H} = \sum_{k=1}^{N}\left[\frac{\hat{\vec{p}}_{\text{k}}^{\,2}}{2} - \frac{1}{2c}\vec{A}\cdot\hat{\vec{p}}_{\text{k}} + \frac{1}{2c^2}\vec{A}^2\right] + V \quad (2.4)$$

V stands as a shorthand for the electron nucleus as well as for the electron−electron interaction potential, and $\hat{\vec{p}}_{\text{k}}$ is the momentum operator. $\vec{A}$ is the vector potential of the external magnetic field, for which the Coulomb gauge

$$\vec{A}(\vec{r}) = \frac{1}{2}\,(\vec{B} \times \vec{r}) \quad (2.5)$$

is chosen. Furthermore, it has been considered that $\vec{\nabla}\cdot\vec{A} = 0$. Consideration of only linear terms in the magnetic field ("weak perturbation"), the perturbation operator of the external magnetic field $\hat{H}^{(1)}$ ($\hat{H} = \hat{H}^{(0)} + \hat{H}^{(1)}$) is given by:

$$\hat{H}^{(1)} = -\frac{i}{2c}\,(\vec{B}_{\text{ext}} \times \vec{r})\cdot\vec{\nabla} = \frac{1}{2c}\,\vec{B}_{\text{ext}}\cdot\vec{L} \quad (2.6)$$

where $\hat{\vec{L}}$ denotes the angular momentum operator.

The current density $\vec{j}(\vec{r})$ may be expanded in a Taylor series in $\vec{B}_{\text{ext}}$:

$$\vec{j}(\vec{r}) = \vec{j}^{(0)}(\vec{r}) + \vec{j}^{(1)}(\vec{r}) + \ldots$$

$$\vec{j}^{(1)}(\vec{r}) = \vec{B}_{\text{ext}}\vec{\vec{j}}^{(1)}(\vec{r}) \text{ with } (\vec{\vec{j}}^{(1)}(\vec{r}))_{\alpha\beta} = \frac{\partial(\vec{j}(\vec{r}))_\alpha}{\partial(\vec{B})_\beta} \quad (2.7)$$

where $\vec{j}^{(1)}(\vec{r})$ is the current density in a molecule without external magnetic field. It vanishes for molecules without a permanent magnetic moment. With a corresponding expansion of the wave function:

$$\Psi_0(\vec{B}_{\text{ext}}) = \Psi_0^{(0)} + i\,\vec{B}_{\text{ext}}\cdot\vec{\Psi}_0^{(1)} + \ldots \quad (2.8)$$

the current density up to linear terms in the magnetic field may then be written as:

$$\vec{B}_{\mathrm{ext}} \cdot \overset{\rightrightarrows}{j}^{(1)}(\vec{r}) = \frac{i}{2}\Big\{\vec{B}_{\mathrm{ext}}\Big[\Psi_0^{(0)}(\vec{\nabla} \cdot \vec{\Psi}_0^{(1)}) - \vec{\Psi}_0^{(1)} \cdot (\vec{\nabla}\Psi_0^{(0)}) - \frac{1}{c}\vec{A}\left|\Psi_0^{(0)}\right|^2\Big]\Big\} \quad (2.9)$$

Using only these linear terms in Biot–Savart's law, one obtains for the shielding function:

$$\overset{\rightrightarrows}{\sigma}(\vec{r}_{\mathrm{k}}) = \frac{1}{2c}\left\langle \Psi_0^{(0)} \left| \frac{(\vec{r} \cdot \vec{r}_{\mathrm{k}})\overset{\rightrightarrows}{I} - \vec{r}_{\mathrm{k}} \otimes \vec{r}}{r_{\mathrm{k}}^3} \right| \Psi_0^{(0)} \right\rangle - \frac{2}{c}\left\langle \Psi_0^{(0)} \left| \frac{\hat{\vec{L}}}{r_{\mathrm{k}}^3} \right| \vec{\Psi}_0^{(1)} \right\rangle \quad (2.10)$$

where $\overset{\rightrightarrows}{I}$ denotes the identity matrix. As for the NMR shielding tensors, the first term is called the diamagnetic contribution to $\overset{\rightrightarrows}{\sigma}$, whereas the second term is called the paramagnetic contribution.

The first-order perturbed wave function $\vec{\Psi}_0^{(1)}$ is traditionally expanded in terms of excited states of the unperturbed system:

$$\vec{\Psi}_0^{(1)} = \sum_{n \neq 0} \vec{C}_n^{(1)} \Psi_n^{(0)} \quad (2.11)$$

This leads to the same expressions as originally derived for the NMR shielding tensors by Ramsey,[1] when $\vec{r}_{\mathrm{k}}$ is restricted to the nuclear positions $\vec{r}_{\mathrm{k}} = \vec{R}_{\mathrm{k}}$:

$$\overset{\rightrightarrows}{\sigma}(\vec{r}_{\mathrm{k}}) = \frac{1}{2c^2}\left\langle \Psi_0^{(0)} \left| \frac{(\vec{r} \cdot \vec{r}_{\mathrm{k}})\overset{\rightrightarrows}{I} - \vec{r}_{\mathrm{k}} \otimes \vec{r}}{r_{\mathrm{k}}^3} \right| \Psi_0^{(0)} \right\rangle - \frac{2}{c}\sum_{n \neq 0} \frac{1}{E_n - E_0}\left\langle \Psi_0^{(0)} \left| \frac{\hat{\vec{L}}}{r_{\mathrm{k}}^3} \right| \Psi_n^{(0)} \right\rangle \otimes \langle \Psi_n^{(0)} | \hat{\vec{L}} | \Psi_0^{(0)} \rangle \quad (2.12)$$

Calculations of the shielding function using eq 2.12 would require the knowledge of the complete set of the solutions of the unperturbed (without external magnetic field) many-particle Schrödinger equation $\Psi_0^{(0)}, \Psi_1^{(0)}, \Psi_2^{(0)}, \ldots$ with the corresponding energies $E_0^{(0)}, E_1^{(0)}, E_2^{(0)}, \ldots$

However, concerning the Coulomb interactions between the electrons, only approximate solutions of the Schrödinger equation can be obtained in principle. Within the Hamiltonian of eq 2.4, the magnetic field acts only in the kinetic energy part. Therefore, one might expect that the shielding function can simply be calculated by application of eq 2.12, just by using approximate solutions for $\Psi_0^{(0)}, \Psi_1^{(0)}, \Psi_2^{(0)}$, ... and $E_0^{(0)}, E_1^{(0)}, E_2^{(0)}$, ... However, even in the single determinant (Slater determinant) ansatz for the wave function (HF), it turns out that the problem is more involved. Within HF theory, the single particle wave functions (orbitals) ψ_j of the Slater determinant are solutions of single particle-like equations (HF equations):

$$\hat{F}\psi_j = \epsilon_j \psi_j \quad (2.13)$$

The Fock operator, $\hat{F}$, the orbitals, ψ_j, and the orbital energies, ϵ_j, can be expanded in a Taylor series similar as in eq 2.8:

$$\psi_j = \psi_j^{(0)} + i\,\vec{B}_{\mathrm{ext}} \cdot \vec{\psi}_j^{(1)} + \ldots$$
$$\epsilon_j = \epsilon_j^{(0)} + i\,\vec{B}_{\mathrm{ext}} \cdot \vec{\epsilon}_j^{(1)} + \ldots$$
$$\hat{F}_j = \hat{F}_j^{(0)} + i\,\vec{B}_{\mathrm{ext}} \cdot \hat{\vec{F}}_j^{(1)} + \ldots \quad (2.14)$$

$\hat{F}^{(0)}$ is the Fock operator without an external magnetic field

$$\hat{F}^{(0)} = \frac{\hat{\vec{p}}^2}{2} + V_{\mathrm{ext}} + \sum_{j=1}^{N_{\mathrm{occ}}} (2J_j^{(0)} - K_j^{(0)}) \quad (2.15)$$

where V_{ext} stands for the scalar external potential (electron nucleus potential) and $J_j^{(0)}$ and $K_j^{(0)}$ are the usual Coulomb and exchange expressions, respectively. The first-order perturbed Fock operator $\hat{\vec{F}}^{(1)}$ is, however, not only given by $\hat{H}^{(1)}$ (eq 2.6). There is no first-order correction to J_j, but there has to be considered one in the exchange part K_j:

$$\hat{\vec{F}}^{(1)} = \vec{B}_{\mathrm{ext}}\hat{H}^{(1)} - \sum_{j=1}^{N_{\mathrm{occ}}} \vec{K}_j^{(1)} \quad (2.16)$$

$$\vec{K}_j^{(1)}\psi(\vec{r}) = \int [\vec{\psi}_j^{(1)}(\vec{r})\psi_j^{(0)}(\vec{r}\,') - \psi_j^{(0)}(\vec{r})\vec{\psi}_j^{(1)}(\vec{r}\,')]\, \frac{1}{|\vec{r} - \vec{r}\,'|}\psi(\vec{r}\,')\, \mathrm{d}^3r' \quad (2.17)$$

Inserting expansions (2.13) into eq 2.13, one obtains up to first order a set of linear equations, which has to be solved successively:

$$(\hat{h}^{(0)} - \epsilon_j^{(0)})\psi_j^{(0)} = 0 \quad (2.18)$$

$$i(\hat{h}^{(0)} - \epsilon_j^{(0)})\,\vec{B}_{\mathrm{ext}} \cdot \vec{\psi}_j^{(1)} = [\vec{B}_{\mathrm{ext}} \cdot (\vec{\epsilon}_j^{(1)} - \hat{\vec{F}}^{(1)})]\psi_j^{(0)} \quad (2.19)$$

Because of the exchange part, the first order perturbed eq 2.19 has to be solved iteratively –CHF.[3]

In principle, DFT is not appropriate to calculate shielding functions, because the Hohenberg–Kohn theorem[27] does not consider external magnetic fields. However, Rajagopal and Callaway[29] derived a relativistic generalization of the Hohenberg–Kohn theorem, which includes also external magnetic fields. That is, the ground state energy of a many-particle system in an external static field, given by the four-component vector potential A_μ^{ext}, is a unique functional of the four-component current density j_μ:

$$E[\mathrm{j}_\mu] = F[\mathrm{j}_\mu] - e\int \sum_{\mu=0}^{3} \mathrm{j}_\mu A_\mu^{\mathrm{ext}}\, \mathrm{d}^3r \quad \text{with } A_\mu^{\mathrm{ext}} = (V_{\mathrm{ext}}, \vec{A}_{\mathrm{ext}}) \quad (2.20)$$

V_{ext} denotes the scalar external potential and $\vec{A}_{\mathrm{ext}}$ denotes the external vector potential. The zero-th component of j_μ is directly related to the ground state charge density ρ, while the other three components are given by the displacement current $\vec{I}$, the spin density $\vec{S}$, and m_{e} is the electron mass. (In our notation, a vector arrow describes the indices 1, 2, and 3.)

$$\mathrm{j}_\mu \leftrightarrow \begin{cases} j_0 = \dfrac{\rho}{e} \\ \vec{j} = \vec{I} + \dfrac{1}{2m_\mathrm{e}}\vec{\nabla} \times \vec{S} + \dfrac{\mathrm{d}\vec{G}}{\mathrm{d}t} \text{ for } \mu = 1, 2, 3 \end{cases} \tag{2.21}$$

The time derivative of the ground state $\mathrm{d}\vec{G}/\mathrm{d}t$ in eq 2.21 vanishes for a time-independent ground state. In analogy to Kohn and Sham,[28] eq 2.20 may be written as:

$$E[\mathrm{j}_\mu] = T\,[\mathrm{j}_\mu] - \frac{e}{2}\int \sum_{\mu=0}^{3} \mathrm{j}_\mu a_\mu^\dagger E_\mathrm{xc}\,[\mathrm{j}_\mu]\,\mathrm{d}^3x + e\int \sum_{\mu=0}^{3} \mathrm{j}_\mu A_\mu^\mathrm{ext}\,\mathrm{d}^3x \tag{2.22}$$

T denotes the kinetic energy of the noninteracting system, and E_xc denotes the exchange and correlation energy. Coordinates are given now in spin-dependent notation $\vec{x} = (\vec{r}, s)$.

The a_μ is the counterpart to the nonrelativistic mean field potential $a_\mu = \langle \Psi_{\vec{B}} | \hat{A}_\mu | \Psi_{\vec{B}} \rangle$, where $\hat{A}_\mu$ is the field operator of the four potential, which is created by the electronic system, and $\Psi_{\vec{B}}$ is the ground state of the system with N electrons in the presence of an external field $\vec{B}_\mathrm{ext}$. In analogy to the nonrelativistic case,[7] a variational ansatz for j_μ can be applied

$$\begin{aligned} \mathrm{j}_\mu &= \sum_{j=1}^{N} \bar{\psi}_j \gamma_\mu \psi_j \\ \bar{\psi} &= \psi^* \beta \\ \gamma_\mu &\leftrightarrow \begin{cases} \gamma_0 = \beta \\ \vec{\gamma} = \beta\vec{\alpha},\ \mu = 1, 2, 3 \end{cases} \end{aligned} \tag{2.23}$$

N is the number of electrons, ψ denotes now, in the relativistic case, the four-component Dirac wave function, and $\vec{\alpha}$ and β are the Dirac matrices with $\beta = \alpha_0$. This leads to effective one particle equations:

$$[-i\vec{\alpha} \cdot \vec{\nabla} + \beta m_0 + e\sum_{\mu=0}^{3} \gamma_0 \gamma_\mu (A_\mu^\mathrm{ext} + a_\mu + a_\mu^\mathrm{xc})]\psi_j = \epsilon_j \psi_j \tag{2.24}$$

where $e \cdot a_\mu^\mathrm{xc}$ is the XC four-component potential

$$e a_\mu^\mathrm{xc} = \frac{\partial E_\mathrm{xc}}{\partial \mathrm{j}_\mu} \tag{2.25}$$

The equations (2.24) are generalizations of the well-known Kohn–Sham equations,[28] accounting for all relativistic effects and the possible presence of an external magnetic field. Equation 2.24 becomes the usual Dirac equation in an external magnetic field in the one-particle case. The detailed derivation and discussion of eq 2.24 can be found in the literature.[31,73] Equation 2.24 may be written also with three-component vectors:

$$[\vec{\alpha}(-i\vec{\nabla} - e\vec{A}_\mathrm{eff}) + \beta(m_\mathrm{e} c + V_\mathrm{eff})]\psi_\mathrm{k} = \epsilon_\mathrm{k}\psi_\mathrm{k} \tag{2.26}$$

$$\begin{aligned} \vec{A}_\mathrm{eff} &= \vec{a} + \vec{a}_\mathrm{xc} + \vec{A}_\mathrm{ext} \\ V_\mathrm{eff} &= V_\mathrm{H} + V_\mathrm{xc} + V_\mathrm{ext} \\ V_\mathrm{xc} &= a_0^\mathrm{xc} \end{aligned}$$

V_H is the Hartree potential. In the nonrelativistic limit, taking in the wave function ψ_k only terms of the order of $1/c$, eq 2.26 becomes

$$\left[\frac{1}{2m}\left(-i\vec{\nabla} - \frac{e}{c}\vec{A}_\mathrm{eff}\right)^2 + \frac{e}{2mc}\,\vec{\sigma} \cdot \vec{B}_\mathrm{eff} + V_\mathrm{eff}\right]\psi_\mathrm{k} = \epsilon_\mathrm{k}\,\psi_\mathrm{k} \tag{2.27}$$

where $\vec{\sigma}$ denotes the Pauli spin matrices. Note that eq 2.27 is given in usual units of quantum electrodynamics, where $m_\mathrm{e} = e = h = 1$. The rest energy, mc^2, has been subtracted in eq 2.27.

Equation 2.27 is formally of Pauli type, with the "large component" φ_k of the bispinors ψ_k. We use here the nonrelativistic limit in the one-particle equations. The effects of the electron–electron interaction are contained in eq 2.27 via $\vec{a}_\mathrm{xc}$, $\vec{a}$, and V_H, and all of these terms depend on the charge density, the current density, and the spin density. Therefore, the equations have to be solved iteratively in an SCF scheme. According to expressions for V_xc, see, for example, ref 74, and for $\vec{a}_\mathrm{xc}$, see ref 31. For a more detailed description, see ref 73.

The direct solution of eq 2.27 would give ψ_j in all orders of $\vec{B}_\mathrm{ext}$, while only linear terms in j_μ are necessary for the calculation of $\vec{\vec{\sigma}}(\vec{r})$ (see eq 2.10). Thus, a similar first-order perturbation treatment as for the HF method in $\vec{B}_\mathrm{ext}$ is possible (see eq 2.14).

The perturbed wave function $\varphi_\mathrm{k}^{(1)}$ may also contribute to $\vec{a}$ and to $\vec{a}_\mathrm{xc}$. This "coupling" makes an iterative solution of the perturbation problem necessary—similar to the coupled HF perturbation treatment.[3] The neglect of these "coupling" terms ($\vec{a}_\mathrm{xc} = 0$, $\vec{a} = 0$) leads to an uncoupled perturbation method (UCP). In this case, and under consideration that for diamagnetic systems the matrix element of the ground state with $\vec{\vec{\sigma}} \cdot \vec{B}_\mathrm{ext}$ vanishes, $\vec{h}^{(1)}$ simplifies to the form as given in eq 2.6.

3. Special NMR Properties of Aromatic Molecules

The term "aromaticity", used to describe a molecule, was initially associated with certain properties (in particular with "smell" or "perfumed"), structural characteristics, and chemical reactivity. In the 1930s, Hückel could explain the particular stability of aromatic systems for the first time by using quantum mechanics. The result of this theory for monocyclic rings ([n]annulenes) was Hückel's magic $4n + 2$ π-electrons rule.[75–77] Later, Pauling introduced the ring current concept semiclassically to account for the high diamagnetism and magnetic anisotropy of benzenoid aromatic hydrocarbons.[78] London further suggested a quantum mechanical treatment that successfully correlated with experimental data.[4] The ring current model[4,78,79] has also been used by Pople to account for various NMR chemical shifts.[80] Indeed, a diamagnetic ring current causes considerable downfield shifts (deshielding) in the molecular plane outside the ring and even larger upfield shifts (shieldings) inside.[80,81]

The concept of a ring current, induced by an external magnetic field, has been widely used to interpret properties of aromatic molecules. In more recent times, when such computations became feasible, several groups have been motivated to investigate current density maps, plotted in or parallel to the ring plane of molecules.[82−86] The ARCS approach is a direct consequence of the ring current model.[87] The ring current generated in aromatic molecules by an external field is the origin for a particular magnetic response, which results in special values for other magnetic criteria, as "exalted" magnetic susceptibilities, NMR chemical shifts displaced from their normal ranges, and large shielding values in or above ring planes, mostly referred to as NICS.[60] For a detailed overview, the reader is referred to a special issue of *Chemical Reviews* devoted to aromaticity.[88]

In the context of the ring current model, the mobile π-electrons of benzene will move in an orbit of approximate circular shape. The induced field has a toroidal topology, when applying a magnetic field $\vec{B}_{\mathrm{ind}}$ perpendicular to the plane of the molecule. Considering large rings, such as the [18]annulene (see Scheme 1), which is sufficiently large to have inner hydrogens, it is experimentally observed that those inner hydrogens are even more shifted upfield (−2.99 ppm) than usual outer hydrogens, which are shifted downfield (+9.28 ppm) in aromatic molecules.[81,89,90] These observations render NMR chemical shift criteria particularly suitable for analyzing aromaticity.

Scheme 1. Structure of [18]Annulene $C_{18}H_{18}$

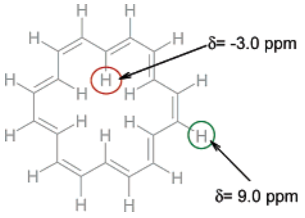

However, the question of the validity of the ring current model to rationalize the strongly shielded protons of benzene has been challenged recently by Wannere and Schleyer[91] and shortly further rightly defended by Zanasi, Lazzeretti, and Viglione.[92,93] Recently, Pelloni, Ligabue, and Lazzeretti also proposed a refined ring current model starting from the differential Biot−Savat law.[94] Detailed analysis of the isotropic chemical shift contributions to the proton shifts of benzene shows that the hydrogen atoms are located inside the shielding rather than the deshielding region.[91] This interpretation is based on the computation of the isotropic shielding and on the analysis of the IMFs of benzene.[95] It is also in agreement with recent quantum chemical calculations of various groups.[59,66,96] On the other hand, the benzene downfield proton chemical shifts are a consequence of the ring currents induced within the π-electron cloud by a magnetic field perpendicular to the molecular plane and the validity of the ring current model can be defended by focusing on the π-contributions to the out-of-plane component of the shielding tensor.[92,93] The refined ring current model of Lazzeretti et al. interprets the "abnormal" proton shifts of benzene (downfield) and cyclobutadiene (upfield) as a result of two opposing elemental IMFs ($d\vec{B}_{\mathrm{ind}}$), induced from opposite sites of the current loop (see Figure 1).[94]

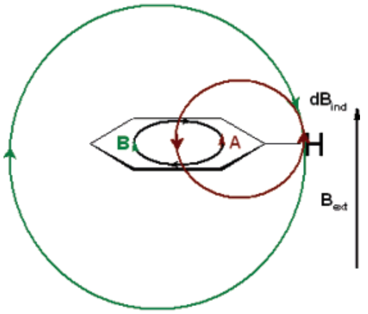

Figure 1. Ring current model for benzene from the Biot−Savart law. The external magnetic field $\vec{B}_{\mathrm{ext}}$ perpendicular to the molecular *xy* plane induces a diamagnetic (clockwise) current density in the π-electrons. The π-current through point A (B) generates an elemental magnetic field $d\vec{B}_{\mathrm{ind}}$, red (green) line, reinforcing (diminishing) $\vec{B}_{\mathrm{ext}}$ at the site of the H proton, and causes deshielding (shielding) by lowering (enhancing) the out-of-plane component $\sigma_{zz}(\vec{r}_{\mathrm{H}})$. Note, however, that the contributions of the σ−electrons are not included in this model. Reprinted with permission from ref 94. Copyright 2004 American Chemical Society.

While the proton chemical shifts are directly accessible in NMR experiment, they have the disadvantage that they are only an indirect indication of electron delocalization effects—The ring current contribution to the proton shielding is small as compared to the contributions of the σ-bonded electrons.[91] A site in the center of the molecule should experience the largest contribution of a ring current and, if no nuclei are in its vicinity, be undisturbed by influences of localized electrons. Therefore, Schleyer, Maerker, Dransfeld, Jiao, and Hommes proposed to compute the shielding in and above ring centers and introduced the NICS[60] index as a probe of aromaticity. The NICS index is the negative value of the isotropic magnetic shielding computed at chosen points in the vicinity of molecules and, hence, directly related to the shielding function of eq 2.12. They are typically computed at ring centers, at points above, and even on grids in and around the molecule. NICS-based techniques are the most widely applied methods used to characterize aromatic molecules. Significantly negative NICS values in interior positions of rings or cages indicate the presence of induced diatropic ring currents, interpreted as "aromaticity", whereas positive values denote paratropic ring currents and "antiaromaticity". Some concerns have been expressed by experimentalists and theoreticians, regarding the use of a "virtual" quantity (NICS) to evaluate such an intangible quantity as aromaticity.[84,97,98] Also, several estimations introducing probe atoms can address the lack of experimental validation of NICS.[61,99−104] A more detailed article in this special issue is devoted to the NICS-based indices and related applications.[105]

As discussed above, the special magnetic properties of aromatic molecules are associated with a ring current in planes parallel to the molecule arising from the π-electrons. In terms of Hückel theory, the π-electrons form a quantum mechanical subsystem, which is mainly decoupled from the σ-system and stabilizes the aromatic molecule. The high degree of delocalization of the π-electrons can be rationalized by electrostatic considerations: The π-electrons experience a molecular electrostatic potential of all nuclei and all core and σ-electrons. In this case, the electrostatic interaction is shielded by the σ-system (as most π-electrons have higher energies than all σ-electrons), resulting in a smooth electrostatic potential as compared to that experienced by the σ-electrons. With these basic arguments, one can rationalize the good performance of rather simple models to describe selected π-systems, as the particle in a box model for annulenes in text books (see, for example, ref 106) or the Jellium model applied to the π-system of fullerenes.[107−109] The most prominent model, which treats the separated π-electrons in a simplified LCAO scheme, is the Hückel theory.[75−77] With this theory, quantum mechanics became popular in chemistry, as structural and electronical properties of aromatic molecules could be explained on a sound physical basis.[106] The idea of a separated π-system has been followed also for augmenting several molecular mechanics (MM) approaches with a quantum treatment for π-electrons: Most MM schemes fail to describe correctly systems with π-electron delocalization, as, for example, fullerenes.[110] On the other hand, QM/MM hybrid schemes, which treat the σ-framework classically but the π-system quantum mechanically (see, for example, QCFF/PI[111] or MM4[112]), are able to provide relative energies and geometries, which are in good agreement with those of DFT and ab initio methods. These observations are true even for systems where strict $\sigma-\pi$ separation cannot be applied, as, for example, for fullerenes: Albertazzi et al.[110] showed that the relative energy of a series of C_{40} fullerenes can be described correctly if the π-subsystem is treated quantum mechanically, e.g., by QCFF/PI, semiempirical, DFT, or HF, while various pure MM schemes (including Tersoff and Brenner potentials[113−115]) failed to give a proper energy classification of the isomers. Also for much larger test sets of classical and nonclassical C_{40} fullerenes, QCFF/PI and the all-valence-electron DFTB[116,117] computations lead to the same conclusions on the stability of such cages if they include squares and heptagons in addition to pentagons and hexagons.[118,119]

These observations confirm the outstanding role of the delocalized π-electrons in sp^2-based carbon compounds. However, if the nodal pattern of the π-orbitals of annulenes is compared with that of the low-energy σ-orbitals, it becomes evident that their only difference lies in the additional nodal plane, which coincides with the molecular ring, located in the molecule's σ_h plane[120] (see Figure 2).

It may be convenient to perform computations with localized rather than canonical orbitals, for instance with LMOs, which can be obtained using a unitary transformation—a transformation that does not affect the total wave function—of the occupied canonical MOs. For example, the IGLO approach,[19] but also several ab initio linear scaling schemes (see, for example, refs 121−127), use LMOs instead of canonical orbitals to reduce computational cost. Some localization procedures appear to be "natural", as they produce localized electron pairs, which reveal the character of bonds or lone electron pairs, as those obtained by the "natural bond orbitals" (NBO) approach[128] or by the localization scheme proposed by Pipek and Mezey,[129] which is based on charge separation. For annulenes and PAHs, both approaches produce three subsets of local orbitals: the core orbitals; localized σ-orbitals, each characterizing an individual C−H or C−C bond; and π-orbitals. While the first two sets are well-localized and reflect the symmetry of the molecule, the latter cannot be localized: Usually, the π-electrons are transformed to sets of electron pairs, which, for example in benzene, do not reflect the symmetry of the molecule. In practical applications, this may have the consequence of an artificial symmetry break for computed properties on the basis of such LMOs, especially in the case of NMR−IGLO computations.[130] However, there are localization procedures that perform a joint localization of σ- and π-orbitals, e.g., the Foster−Boys localization scheme,[131−133] which reveals better numerical results.[21]

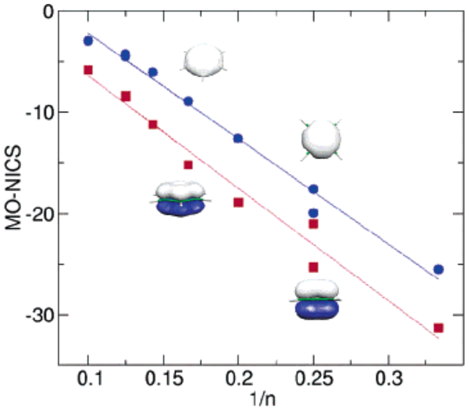

Figure 2. NICS of the lowest molecular orbital (MO) (k = 0) σ-orbitals (red) and π-orbitals (blue) correlate with the inverse number of ring atoms, 1/n for [n] annulenes $C_{10}H_{10}$ to $C_3H_3^+$ from left to right. Reprinted with permission from ref 120. Copyright 2003 American Chemical Society.

To conclude, the special properties of aromatic molecules are a direct consequence of the delocalized π-systems of these compounds. In benzoid aromatics, usually half of the π-orbitals are occupied, these are all binding states given by Hückel theory. The larger the ring, the lower is the π-stabilization energy per carbon.[89,90,106,134] The π-stabilization energy competes with additional σ-strain: Benzene is hence the perfect aromatic molecule, as its C−C−C bond angles fit perfectly the 120° angle of the sp^2-hybridized orbitals. Larger and smaller rings than benzene suffer from stronger σ-strain and are therefore less stable. Hence, it is not surprising that benzene and its derivates cover by far the largest amount of aromatic monocycles, followed by the cyclopentadiene anion. In all aromatic molecules, the π-orbitals determine the frontier orbitals and, hence, their reactivity and optical properties, which again allow the computation of such properties using Hückel theory or other computational schemes restricted to the quantum mechanical description of the π-electrons. A very prominent representative of this family of methods, aiming at the computation of optical properties, is the Pariser–Parr–Pople -method.[135–138]

4. Magnetically Induced Current Densities and Related Models

A detailed review on ring current models and methods, starting from the formulation of the problem by Pauling,[78] Londsdale,[79] and London,[4,139,140] up to the ab initio computation of the topology of the ring current density field,[141] and highlighting the theoretical backgrounds of each approach, has been given by Lazzeretti in 2000.[84] This review covers the whole range of theoretical work from the early formulation of the method, the introduction of ring current models, semiempirical computations of ring currents and properties arising from ring currents, until it discusses in detail the more recent ab initio based current density approaches. The analysis of the global current density of a molecule induced by an external field goes back to Gomes' work in the 1980s.[142–146] Such studies became more popular after the introduction of the ipsocentric approach, based on a CSGT[25,147] or, similarly, on a CTOCD.[26,148] The latter has been the most popular method to compute current density maps.[149–165] In this approach, the gauge transformation problem is resolved by using a different gauge origin for each point for which the current density is calculated. Within the CTOCD-DZ variant, the gauge origin is identical to the point at which the current density is computed,[26,148] while in the CTOCD-PZ alternative the gauge origin is chosen such that the transverse component of the paramagnetic current density is annihilated.[85,165,166] The latter method has been applied recently to a large series of molecules by Steiner, Fowler, and coworkers.[149,150,152–164]

While the diamagnetic and paramagnetic contributions to the current density in eq 2.1 are origin-dependent and have no separate physical significance, the total current can exhibit diamagnetic or paramagnetic behavior in terms of the direction of the magnetic field generated by the current in the region encompassed by the trajectories. Maps of magnetically induced current densities in molecules were first illustrated by Lipscomb and others.[3,167–169]

The topological analysis of the current density was proposed in 1983 by Gomes[142–146,170] and in more detail, including the evaluation of basins, 10 years later by Keith and Bader.[147] Before discussing the physics of the ring current density, we briefly recall what can be extracted from a topological analysis of the electron density (see Figure 3). For a detailed review of topological analysis of various quantities related to the current density, we refer to Merino et al.[171]

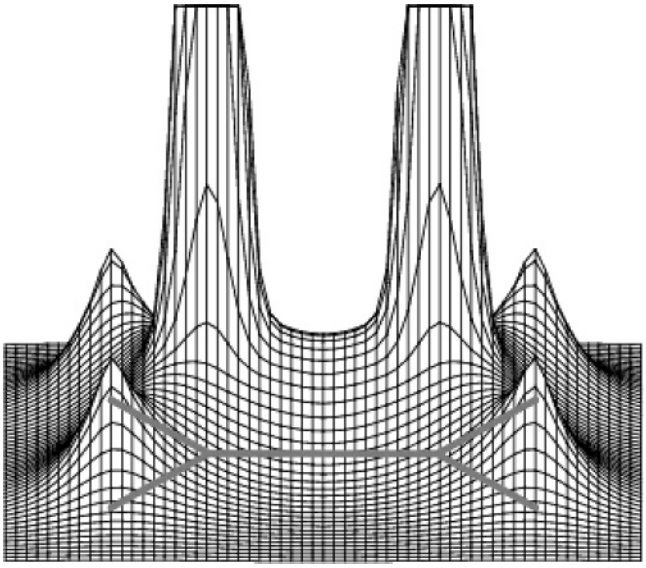

Figure 3. Electron density $\rho(\vec{r})$ in a plane containing the two carbon and four hydrogen nuclei of the ethene molecule. The absolute maxima of $\rho(\vec{r})$ are attained at the positions of the carbon nuclei, and the saddle points, the bond critical points, are located at the bonds.

In a molecule, nuclei act as point attractors immersed in a cloud of negative charge, the electron density $\rho(\vec{r})$. The electron density describes the manner in which the electronic charge is distributed throughout real space. The electron density, which is in principle a measurable property, has a maximum at the position of nuclei and decays rapidly away from these positions. The presence of these local maxima at the positions of the nuclei is the general and also the dominant topological property of $\rho(\vec{r})$.

To extract information on the topology of the molecule from the three-dimensional scalar electron density, one has to determine special regions, points, and surfaces of the density. In particular, the separation of the electron density into basins has led to the concept of atoms-in-molecules,[172] which allows the computation of several quantities and relate them to atomic contributions, as charges,[173,174] polarizabilities,[175] or magnetic response properties.[24,83] These basins are separated by the zero flux surfaces.[176] Zero flux surfaces are interatomic surfaces, which are defined by trajectories of $\vec{\nabla}\rho(\vec{r})$ that terminate at one point and which are not crossed by any other trajectories of $\vec{\nabla}\rho(\vec{r})$. The critical points of the electron density, i.e., the locations $\vec{r}_0$ where $\vec{\nabla}\rho(\vec{r}_0) = 0$, have importance for the interpretation of the chemical bonding. Among others, bond critical points, i.e., first-order saddle points between atoms, and ring critical points, which are second-order saddle points in the topological center of a ring, are distinguished.

When placing a molecule in an external magnetic field, the relevant response property is the current density. The current density is a three-component vector field, and a topological analysis of a vector field differs considerably from that of a scalar field. The most important critical points are singularities for which the magnitude of the current density is zero, also referred to as "stagnation points". The presence of such a stagnation point is necessary for establishing a ring current, but there are several other possibilities of density distributions than ring currents. For a complete mathematical description of this topic, the reader is referred to the milestone papers in the literature[142–144,146,147,170] and two review articles, which deal with this the topological analysis of ring current densities.[84,98]

Whether a region of current flow is diamagnetic or paramagnetic depends on the curl of the current density $\vec{\nabla} \times \vec{j}(\vec{r})$ at the stagnation point, also called its vorticity field, relative to the atomic shell structure. The gradient of the current density is an asymmetric tensor[143,170] and, hence, depends on the choice of the coordinate system. In practice, the topological analysis is connected with a rather cumbersome mathematical procedure necessary to classify the critical points. Keith and Bader showed that a proper choice of gauge origin is essential for the calculation of correct current densities.[25] They also performed the topological analysis of the current density for some example cases.[25,147,177] As the gain of chemical insight, which could be revealed by this analysis, was in no relation to the necessary mathematical efforts for implementing and running the method into chemical standard software, it did not become popular until today. However, the topological analysis of molecular fields recently became an attractive field of research, and it can be expected that the method experiences some renaissance.[171] It also turned out that for delocalized systems information on ring currents and electron delocalization can be gained by studying the current density and its curl. Such investigations, accompanied by an analysis of atomic contributions to the magnetic susceptibility, have been carried out by the same authors for benzene.[25,147,177]

They found out that "the curl of the current density map mimics not only (the Laplacian of the electronic density) $\Delta\rho(\vec{r})$, but also its bonding features": The vorticity field clearly shows three basins around each carbon atom, which are describing its three σ-bonds (Figure 4c,d). Keith and Bader also point out in their analysis of atomic contributions to the magnetic susceptibility of benzene that "the shape of the current plot and the relative basin to surface contributions to the mean susceptibility of the carbon atoms confirm the existence of a significant diamagnetic current encompassing the ring of the benzene molecule."[25] The current density in the molecular plane reflects the shape of the benzene framework, while at 0.8 Å above the molecular framework, ring currents, whose center is the origin of the plane, are observed. The current density perpendicular to the plane, cutting through a C−H bond, is reflecting the shape of the carbon p_z orbitals and the presence of a substantial paramagnetic current localized in the basins of the carbons.

Keith and Bader also discuss the large anisotropy of the magnetic susceptibility as a direct consequence of the delocalized nature of the current, which is induced by a current that is parallel to the molecular plane.[25] The concept of anisotropy of the magnetic susceptibility is, however, limited, as it requires a choice of a plane to which the anisotropy needs to be defined.[178] For planar systems, the choice is natural, but for general molecules, the choice might be rather arbitrary. Therefore, in 2001, Herges and Geuenich introduced the ACID concept. They compute the anisotropy A of a tensor T, which is related to applied magnetic field and current density[178] and which is hence in close relation with the magnetic susceptibility:

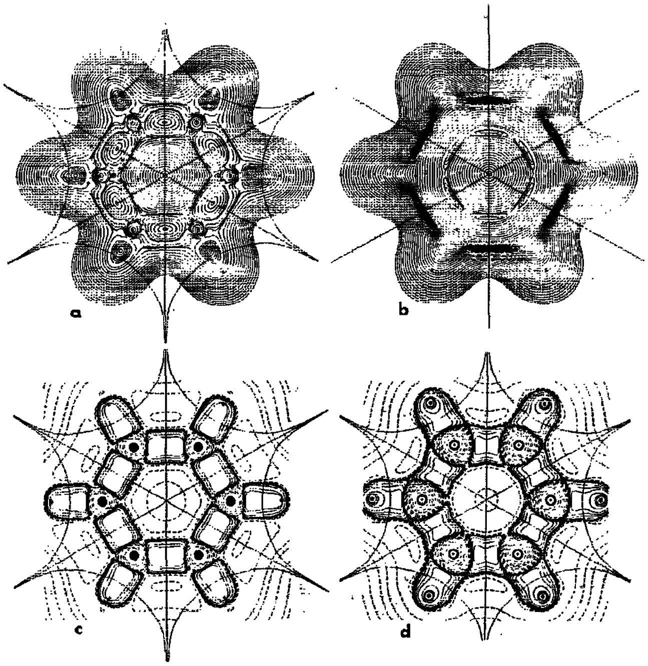

Figure 4. Displays of the current density, its curl, and the Laplacian of ρ for the benzene molecule in the plane containing the nuclei. The maps for the current density and its curl are for a field directed out of and perpendicular to the plane. In part a, the current density is shown in the symmetry plane. Part b is a projection onto a plane 0.8 au above the symmetry plane of the trajectories, which intersect it. In addition to the outer diamagnetic and inner paramagnetic flows, there is a vestige of each bonded set of diamagnetic current flows present. The shell structure and regions of charge concentration/depletion defined by the Laplacian of the density in part d are similar to the shell structure and regions of outwardly/inwardly directed flux in the curl of the current density field in part c. Reprinted with permission from ref 177. Copyright 1993 American Institute of Physics.

$$A = tr(T^2) + \frac{1}{3}[tr(T)]^2$$

$$T_{\alpha\beta} = \left.\frac{\partial j_\alpha}{\partial B_\beta}\right|_{B=0}$$

The ACID is a scalar field, which can be visualized easily. Herges and Geuenich discuss the symmetry properties of ACID in great detail and show that "for closed shell molecules in the ground state the ACID isosurface has the same symmetry as the molecule." Furthermore, they point out that "this is different from the current density itself which is of the same symmetry as the rotation of one of the Cartesian axes depending on the orientation of the magnetic field. The symmetry properties are another advantage of using the anisotropy of the current density over the current density for the visualization of delocalization." The method has been applied to the series cyclohexane, cyclohexene, cyclohexadiene, and benzene. Figure 5 shows the ACID (yellow) of these molecules. Obviously, delocalized π-bonds exhibit a significant ACID, and for the benzene molecule, the ACID isosurface shows a closed ring. Even though

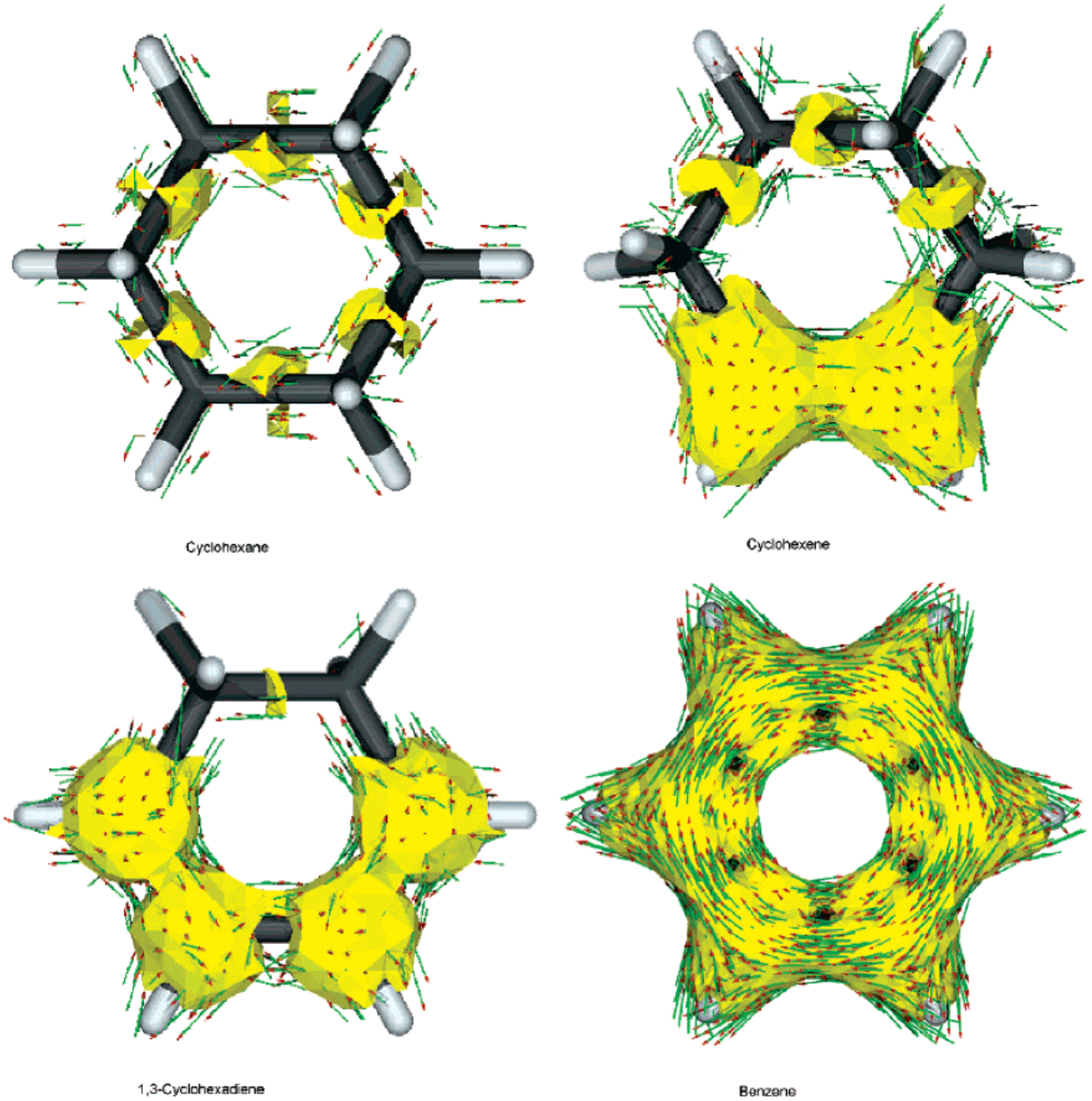

Figure 5. Isosurfaces of the ACID of cyclohexane, cyclohexene, 1.3-cyclohexadiene, and benzene at an isosurface value of 0.05. Current density vectors are plotted onto the isosurface. The vector of the magnetic field is perpendicular to the ring plane (in the case of cyclohexane C_1, C_2, and the midpoint of the C_4-C_5 bond and in cyclohexene C_2, C_3, and the midpoint of the C_5-C_6 bond define an approximate ring plane). Reprinted with permission from ref 178. Copyright 2001 American Chemical Society.

ACID appears to be a reasonable way to address electron delocalization in molecules in a clean, first-principle way, the lack of implementation in popular quantum chemistry software was limiting the application of this approach. It has been applied so far to detect homoaromaticity in Tris(ethylene)nickel(0) and Tris(ethyne)nickel(0) species,[179] to study the electron delocalization of transition states in the cyclization reactions,[180] to understand reaction mechanisms,[181,182] or to discuss the degree of delocalization in biological systems.[183] Another article of this special issue deals in more detail with the ACID analysis.[184]

Both the CSGT and the CTOCD-DZ/PZ approaches have the disadvantage that at each point in space a different gauge transformation has to be applied. Furthermore, NMR computations employing these methods are generally less efficient than the GIAO approach.[185] Therefore, they never have been established as standard working tools for NMR computations of molecules, even though the CSGT method is implemented in most of the widespread quantum chemistry software. The computation of current densities within the GIAO method was proposed by Keith in 1996,[82] but it has been used only for the evaluation of magnetizabilities, which have been found, however, in good agreement with full GIAO computations. Recently, Jusélius, Sundholm, and Gauss proposed a similar approach to calculate gauge-independent magnetic-induced currents (GIMIC),[86] thus applying only one single gauge transformation to the current density of the entire molecule. The obtained current densities are gauge origin-independent, but gauge invariance is achieved only in the limit of complete basis sets.[86] For the application of GIMIC on the basis of correlated ab initio methods, it is worth noting that the resulting expression for the current density is cast in a form that only requires knowledge of the unperturbed and perturbed one-electron density matrices. This gives the

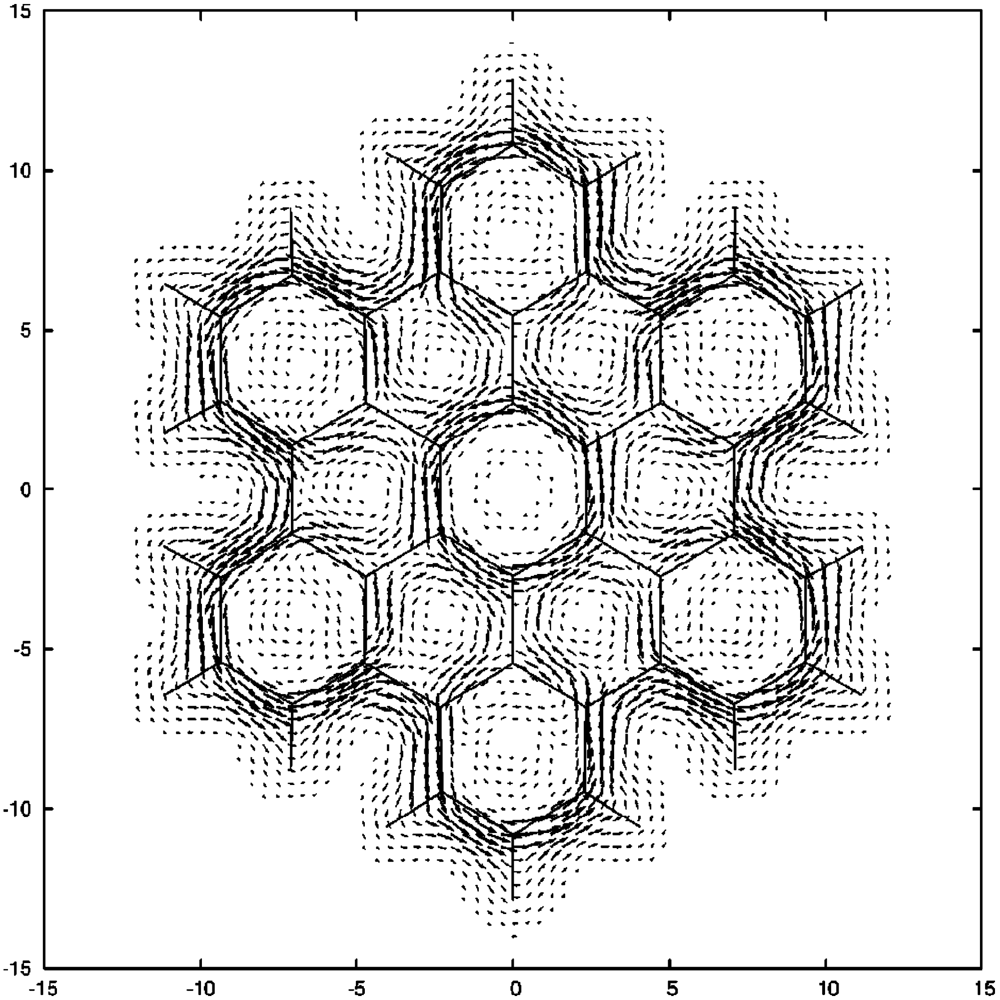

Figure 6. Induced current density for hexabenzocoronene calculated at the DFT-BP86/TZP level. The current density is displayed in a plane parallel to the molecular framework and 1 bohr above it with the magnetic field chosen perpendicular to the molecular plane. Reprinted with permission from ref 86. Copyright 2004 American Institute of Physics.

advantage that current densities can be calculated within this approach at all computational levels for which these one-electron density matrices are available. In practice, this means that it can be applied with computationally inexpensive DFT, which will allow the study of reasonably large systems, but also to highly correlated coupled cluster schemes, which is advantageous if controversial results need to be explored at higher accuracy. The good performance of the method is illustrated by studies of fairly large molecules such as hexabenzocoronene[86] (see Figure 6), arsole, and the C_{60} buckminsterfullerene.[186]

The induced current density of eq 2.1 can, as shown above, be accessed at any level of theory. In practical implementation of NMR codes, however, the shielding tensor is computed directly using the expressions of eq 2.12, and costly application of gauge transformations to the current density itself is avoided. Therefore, the current density information is not directly extractable in most quantum chemistry codes, even though the whole functionality of NMR shielding computations is implemented.

To access a quantity that is directly related to the integrated ring current of an aromatic ring, Jusélius and Sundholm introduced the ARCS approach.[87] Using a simple expression, they related the long-range part of the isotropic magnetic shielding function to the ring current susceptibility and to the size of the aromatic pathway. If the shielding function results from a ring current, its long-range part perpendicular to the ring, $\sigma(z)$ (e.g., from $z = 3$ to 20 Å from the ring plane), provides information about strengths and radius of this ring current. The Biot–Savart law, as expressed in eq 2.2, defines the relation between the long-range behavior of the isotropic magnetic shielding function, $\sigma(z)$, and the ring current susceptibility with respect to the applied magnetic field:

$$\sigma(z) = -\frac{\mu_0}{2}\frac{\partial I_{\mathrm{ring}}}{\partial B_{\mathrm{ext}}}\frac{R^2}{(z^2 + R^2)^{(3/2)}} \qquad (4.1)$$

In eq 4.1, it is assumed that the wire carrying the current is circular and infinitely thin, $\sigma(z)$ corresponds to the shielding function, z defines the perpendicular distance from the center of the current loop, μ_0 is the vacuum permeability, I_{ring} is the current susceptibility, B_{ext} is the perpendicular component of the external magnetic field, and R is the radius of the current loop. Technically, the current susceptibility and the size of the current loop can then be deduced by calculating the shielding function at

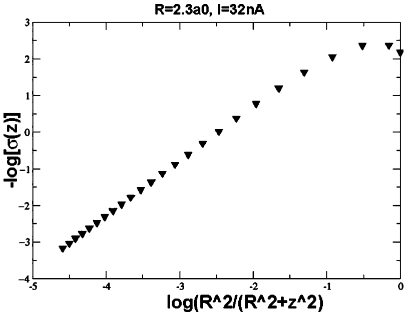

Figure 7. ARCS fit for benzene. The long-range magnetic shielding function $\sigma(z)$ (in ppm) calculated at the IGLO-PW91/IGLOIII level in a homogeneous external magnetic field of 4 T.

many NICS points along the z-axis and by using a logarithmic fit as it is shown in Figure 7 and eq 4.2.

$$-\log\,[\sigma(z)] = \frac{3}{2}\left\{\log\left[\frac{R^2}{z^2+R^2}\right]\right\} + \log\left(\frac{\mu_0 I_{\text{ring}}}{2R\cdot B_{\text{ext}}}\right) \tag{4.2}$$

The ARCS aromaticity index is thus defined by the strength of the ring current susceptibility.

For planar molecules, the current is assumed to circulate in the molecular plane. The shielding contributions due to local currents around the nuclei and in the chemical bonds have small loop radii and decline fast with the distance from the molecule. For nonplanar homoaromatic molecules, the symmetry axis (z-axis) is the one with the largest moment of inertia.[187] However, for nonplanar systems, the ARCS technique is not always able to extrapolate to a finite ring current radius.[188] Finally, for nonaromatic molecules, the shielding practically vanishes outside the electron density. As the effective current radius of aromatic rings is significantly larger, it suggests that the long-range shielding is mainly due to electron delocalization (i.e., the strength of the induced ring current) as confirmed by the analysis of the IMF in molecules[95] (see next section).

The center of the current loop used in the ARCS fit can be estimated from a plot of the ARCS function.[187] For planar molecules, the ring center is the obvious ARCS origin, while for nonplanar molecules, the choice of origin is somewhat arbitrary. However, the ARCS indices are found to be rather independent of the precise location of the ARCS origin. The ARCS method has been applied to annulenes,[87] substituted naphthalene,[188] homoaromatic hydrocarbons,[187] prophyrins,[189,190] Al_4^{2-},[191] and metal organic complexes.[188]

5. Shielding Functions and IMFs of Molecules

Already in 1958, Johnson and Bovey[56] computed the shielding function for benzene as a function of the distance from the ring center and the ring perimeter using a semiempirical formulation restricted to π-electrons. Their motivation was to apply Pauling's ring current model of benzene[78] for the computation of ^{1}H NMR chemical shifts of a series of aromatic compounds by adjusting the geometrical parameters of the computed π-ring current (perimeter and distance from the ring plane). They found excellent agreement with experiment within an accuracy of 0.5 ppm (see Table 1). This work illustrates already the first "isoshielding lines" in the neighborhood of a benzene ring and the long-range nature of the isotropic shielding function in and perpendicular to the ring plane (see Figure 8).

Table 1. Observed and Calculated Positions of Resonance Peaks (in ppm) for Protons in Aromatic Compounds[a]

		shielding values s	
compound	group	observed	calculated
toluene	CH_3	7.66	7.52
ethylbenzene	CH_3	8.80	8.79
cumene	CH_3	8.77	8.79
tetralin	a-CH_2	7.30	7.34
	b-CH_2	8.22	8.07
dibenzyl	CH_2	7.05	7.11
diphenylmethane	CH_2	6.08	6.58
naphthalene	a-CH	2.27	2.03
	b-CH	2.63	2.46

[a] Information is taken from ref 56.

At the *ab initio* level, the shielding function was discussed first in 1979 by Jameson and Buckingham, who introduced the term "magnetic shielding density".[57,58] In a detailed study of the HF molecule, they used the shielding density maps for understanding the chemical bonding of HF as compared to free proton and free F^- ion. They specifically discussed shielding density maps for the isotropic shielding as well as for the principal components of the shielding tensor and its anisotropy, both around the H and F nuclei (see Figure 9), and compared them with the shielding density maps of the free atoms or ions. They expected a large range of application of their approach, but so far, it has only been used for the few examples given by the authors. However, more elaborate computational tools may lead to a renaissance of this methodology, in particular as shielding densities, or very closely related quantities, have been computed recently by quite a few groups, as will be discussed below.

The group of Hansen studied the "molecular magnetic shielding field" of benzene,[59] benzocyclobutadiene,[192] and a Sondheimer aromatic annulene and its nonaromatic analogue.[193] They wrote the shielding function of eq 2.12 (which they call molecular magnetic shielding field) in terms of the LORG formalism[23,194,195] as $\sigma_{\alpha\beta}(\vec{r};\vec{R}_0)$, where $\vec{R}_0$ is the location of gauge origin. They put special emphasis on the graphical representation of the shielding function, for which they employed ellipsoid response graphs, which have been developed by the same group.[196,197] In these graphs, the components of the shielding tensor are transformed to an ellipsoid, and the size of the graphical representation is proportional to the magnitude of the shielding. Such an ellipsoid representation, or alternatively the ovaloid form proposed by Radeglia,[198] is often useful to assign solid state NMR patterns with similar isotropic value, as it allows one to compare the direction of the principal components of the shielding tensor with the molecular axes in a suggestive way. These ellipsoids are drawn into a structure plot of the molecule. The graphical representation of the shielding tensor has

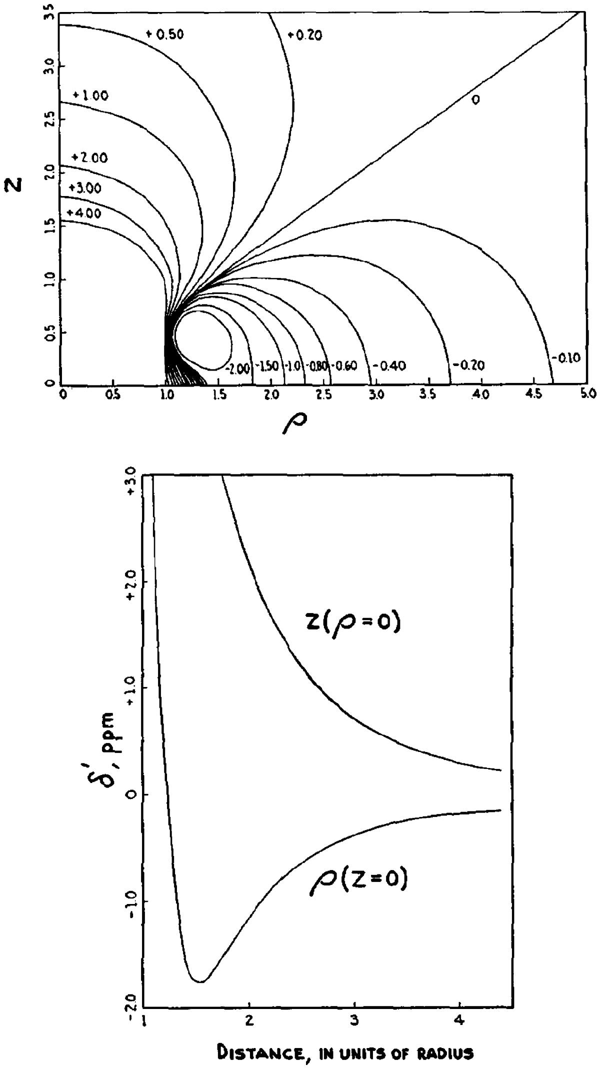

Figure 8. Top: "Isoshielding" lines in the neighborhood of a benzene ring. The plot represents one quadrant of a plane passing normally through the center of the ring. The lines represent the shift in the NMR shielding value, which will be experienced by protons as a result of the magnetic field of the benzene ring. Bottom: The shift δ' in the NMR shielding value for protons in the neighborhood of a benzene ring. Top curve, δ' as a function of distance along the hexagonal axis; bottom curve, δ' as a function of distance from the center of the ring in the plane of the ring. Reprinted with permission from ref 56. Copyright 1958 American Institute of Physics.

been employed for the assignment of ^{1}H NMR chemical shifts in molecules.[193] The axial antisymmetry vectors of the shielding tensor, $\xi_k = 1/2 \sum_{ij} \epsilon_{ijk} \sigma^a_{ij}$, with the alternating tensor ϵ_{ijk} (The antisymmetric tensor ϵ_{ijk}, also called Levi–Civita tensor, is either 1 for even or -1 for uneven permutations of i, j, and k.) and the antisymmetric tensor $\sigma^a_{ij} = 1/2(\sigma_{ij} - \sigma_{ji})$ was used to assess the direction and magnitude of a ring current at a position in the molecular plane. Interesting conclusions were derived using this method: In their study of a Sondheimer aromatic annulene and its nonaromatic analogue[193] (see Figure 10), Hansen and Bilde compared a closed aromatic ring with its open analogue and, surprisingly, found similar ring currents in the molecular plane of both molecules. In other words, "the diamagnetic π-electron contributions are almost insensitive to ring closure and we (Jensen and Hansen[59]) argue that rationalization of the unique magnetic anisotropy of aromatic systems in terms of diamagnetic ring currents seems a misrepresentation of the actual mechanism." In place of "ring current effect", they therefore proposed the term "Pauling–London–Pople effect".[59] In the same work, they opposed the use of the isotropic shielding function at ring centers (that is, NICS) as an index of aromaticity: "The characteristic shielding anisotropy observed for aromatic protons is caused solely by an absence of paramagnetic π electron currents, all other shielding contributions being sensitive to local topology but indifferent to aromatic character."[193] In their study of benzocyclobutadiene,[192] they concluded on grounds of ^{1}H NMR and ring center shielding tensors that this molecule does not qualify for either aromatic or antiaromatic classification. This statement was supported by empiricism,[199] energetics,[200] and valence bond analysis[201] but in disagreement with the aromatic classification of the six-membered ring on energetics[202,203] and NICS values.[60,204] At the time of this study, the question of antiaromaticity of the four-membered ring was left open.[192]

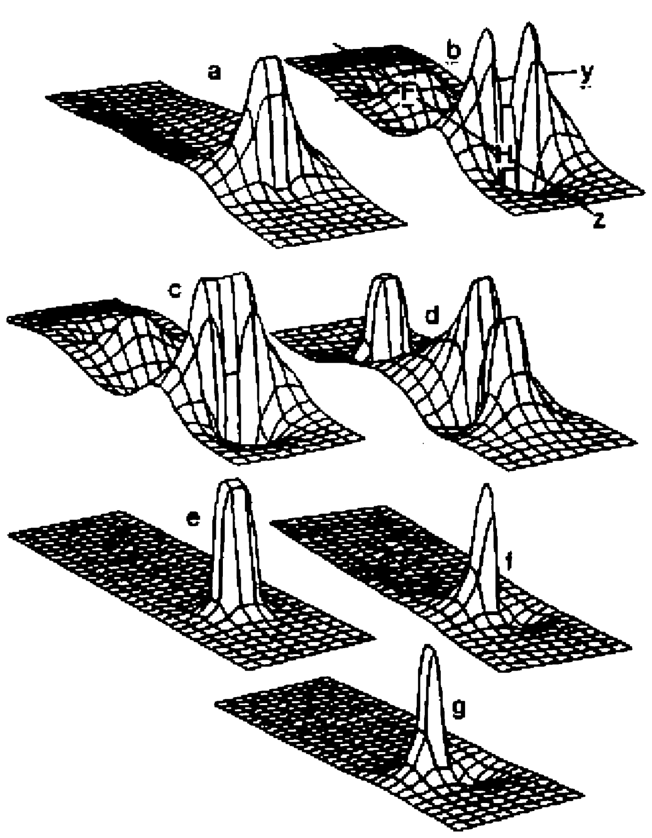

Figure 9. ^{1}H shielding density plots for the HF molecule, with gauge at origin F. The density plots shown are for the $x = 0.0625$ au plane, for the components (a) σ_{zz}, (b) σ_{xx}, (c) $1/3(\sigma_{xx} + \sigma_{yy} + \sigma_{zz})$, (d) $\sigma_{\parallel} - \sigma_{\perp}$, (e) $-\sigma_{xz}$, (f) σ_{yx}, and (g) σ_{yz}. Reprinted with permission from ref 58. Copyright 1980 American Institute of Physics.

The NICS index is the local value of the negative isotropic shielding. After its introduction, the distribution of NICS values on grids around molecules was studied in various cases.[63] These NICS grids are the negative isotropic values of the shielding function (eq

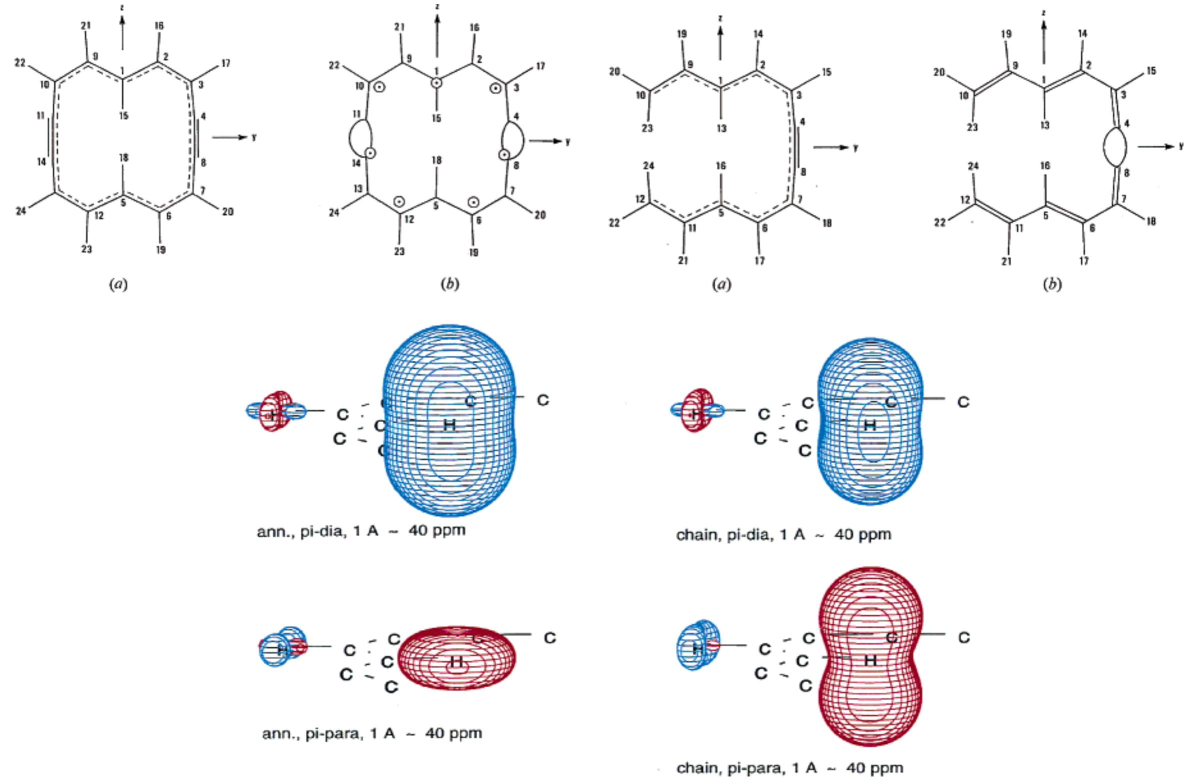

Figure 10. Top left: Structure and coordinate system for 1,8-didehydro[14]annulene: (a) delocalized standard representation and (b) localized bond representation. Right: Structure and coordinate system for the conjugated open chain system: (a) delocalized representation and (b) localized bond representation. Bottom: Shielding graphs for diamagnetic and paramagnetic π-electron shielding contributions for inner and outer protons, $H_{15} + H_{16}$, in annulene (ann.) and $H_{13} + H_{14}$ in the open conjugated chain (chain). The scale is chosen to make 1 Å correspond to 40 ppm. Blue surfaces represent upfield resonances relative to the bare nucleus, and red surfaces represent downfield resonances relative to the bare nucleus. Only the $C_{10}-C_9-C_1-C_2-C_3-C_4-C_8$ fragments of the two structures are shown in the bottom figure. Reprinted with permission from ref 193. Copyright 1997 Taylor and Francis.

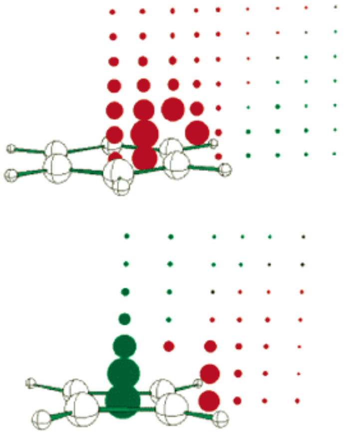

Figure 11. NICS grid of benzene and cyclobutadiene. The red and green colors denote negative and positive NICS values, respectively. The magnitude corresponds to the ring diameter.

2.12) at selected positions around the molecule and provide insight about diatropic and paratropic regions in molecules. Figure 11 shows two typical examples for such NICS grids, aromatic benzene and antiaromatic cyclobutadiene.

In 1997, Wolinski suggested to compute the "magnetic shielding surface" in molecules, a quantity that is identical with the shielding function of eq 2.12.[65] He proposed that this quantity "might be called hypothetical spectroscopy of neutron magnetic resonance", as a "link to NMR spectroscopy can be made by assuming that a neutron virtually moving in a molecule is used as a probe to detect local magnetic fields." He wrote down the shielding function in terms of GIAO, starting from the traditional quantum chemical definition of the shielding tensor of eq 2.12, and finally gave the GIAO formulation of the shielding function. As Jameson and Buckingham 18 years earlier,[57] he studied the shielding function of the HF molecule but also of other small systems such as LiH, LiF, Li_2, HCN, HNC, and HCCH. The main interest was in understanding the distribution of the isotropic shielding values along the molecular axis of these linear molecules. Furthermore, he proposed the idea that the integrated shielding reveals information on the shielding properties of the whole system, but this route has not been followed intensively up to today.

The shape of the isotropic magnetic shielding function also provides information about the delocalization of π-electrons and hence on the molecular aromaticity.[66,96,205] Klod and Kleinpeter[66] computed isosurfaces of the shielding function, so-called ICSSs, with the aim to evaluate the anisotropy effects of double or triple bonds and of aromatic rings. In Figure 12, the increasing π-electron delocalization normal to the ring with respect to the size of a series of PAHs is shown.

The IMF has been used by scientists to understand the magnetism of macroscopic physical objects (e.g., the earth magnetism or electronic devices). Also, chemists applied this concept to understand the

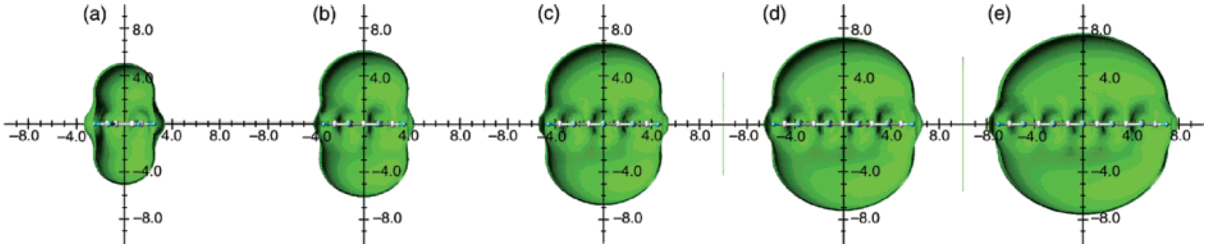

Figure 12. Comparison of the calculated 0.5 ppm shielding surface for annulated aromatic ring systems: (a) benzene, (b) naphthalene, (c) anthracene, (d) tetracene, and (e) pentacene. View in the plane of the molecules. Distances on both axes are given in Ångstroms. Reprinted with permission from ref 66. Copyright 2001 Royal Society of Chemistry.

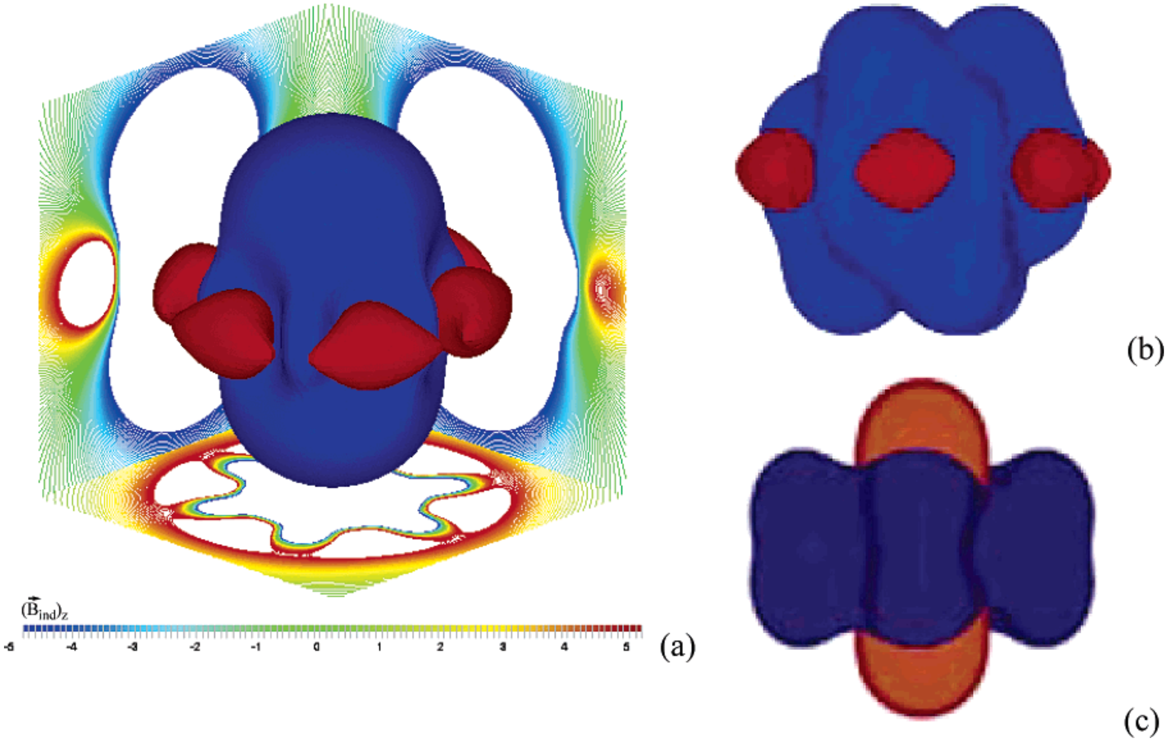

Figure 13. Plot of the 5 ppm isosurface of the *z*-component of the IMF of (a) benzene, (b) cyclohexane, and (c) cyclobutadiene. Contour lines of the *z*-component of the IMF through the molecular center are plotted at the faces of the box. Blue and red indicate shielding and deshielding areas, respectively. Adapted in part with permission from ref 95. Copyright 2004 Wiley-VCH.

magnetic properties of molecules, in particular in the context of NMR.[206] Related electrodynamics quantities, as material constants, are accessible through the IMF and Maxwell's equations. As discussed in section 2, the IMF of a molecule, $\vec{B}_{ind}$, at position $\vec{R}$, can be computed directly from the magnetic shielding function, as given in eq 2.12. The IMF is also related to the current density through Biot−Savart's law, as discussed in section 2 (see eq 2.2). In the Pople ring current model of benzene, discussed in popular NMR textbooks,[206] the Biot−Savart law is applied on a fictitious ring current. Also, in the intensive debate on the applicability of this model, the benzene aromaticity is discussed in terms of a magnetic field induced by projected ring currents.[91,92,94]

The IMF is, however, also directly accessible through the shielding function. By the simple linear relation of eq 2.3, it is computed as the negative product of the shielding tensor with the external (or applied) magnetic field. Hence, the knowledge of the shielding function can be immediately transferred to the induced field. Such a study has been performed recently by Merino, Heine, and Seifert.[95] They showed that the IMF reveals important information on electron delocalization and, furthermore, of its kind: If organic cycles are studied and π-delocalization, or a ring current, is assumed, the external field is pointing perpendicular to the ring. In this case, nonconjugated systems, such as cyclobutane or cyclohexane, only show a short-range response to the magnetic field. In all areas of the molecule except for the immediate vicinity of atoms and bonds, the induced field is small (Figure 13). This is different for conjugated rings: Both antiaromatic D_{2h} cyclobutadiene and D_{6h} benzene show IMFs far away from the molecule and significant contributions in the ring centers. However, the induced fields are either in line with the applied field, hence increasing it (paratropic), for antiaromatic compounds, or against the field, shielding it (diatropic) for aromatic compounds. A detailed analysis of the magnetic field is given in Figure 13 for benzene. In the center, the isosurface of ±5 ppm for the B_z component is given. At the faces of the box, the projected field lines $|\vec{B}_{ind}|$ = const are given for the plane parallel to the face cutting the molecular center. The IMF analysis has been applied recently to understand the electronic properties of compounds containing a planar tetracoordinate carbon,[207] and studies of other systems, including Al$_4^{n-}$ moieties and conjugated double rings, are in progress.

6. Electron Delocalization and Magnetic Response of Example Molecules: Benzene, Cyclobutadiene, and Al$_4^{n-}$

As we have shown in the previous two sections, electron delocalization, especially in cyclic molecules, is conveniently assessed by magnetic criteria, that is, by current densities, by the tensorial shielding function, or by quantities that are directly related to these properties. Although the amount of applications analyzed using the approaches discussed above is enormous, the number of systems that have been studied with all, or at least most of the methods, are rather limited. However, there are four interesting cases, which were studied quite intensively. These are the “aromatic standard” D_{6h} benzene, the “antiaromatic standard” cyclobutadiene, either D_{2h} or forced into D_{4h} symmetry, and forms of the newly synthesized molecules based on planar Al$_4^{2-}$ and Al$_4^{4-}$[208,209] ions (see Figure 14).

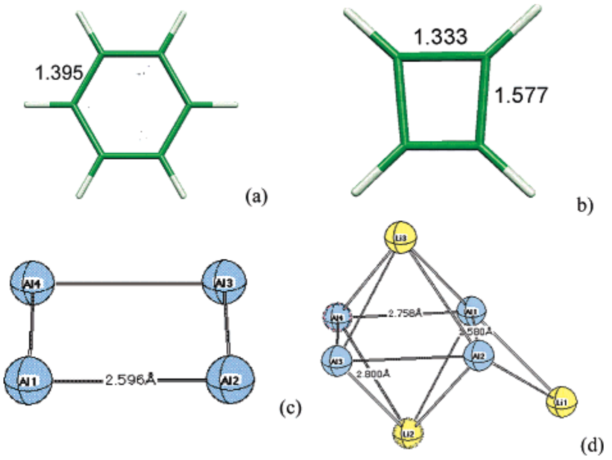

Figure 14. Geometrical parameters of (a) D_{6h} benzene and (b) D_{2h} C_4H_4 at the B3LYP/6-311+G** level and (c) D_{4h} Al$_4^{2-}$ and (d) C_s Al$_4$Li$_3^-$ at the PW91/DZVP level.

Hückel theory can formally be applied to each of these species, as they are all planar and exhibit an electronic π-system. Counting of π-electrons reveals six electrons for benzene, four for cyclobutadiene, two for Al$_4^{2-}$, and four for Al$_4^{4-}$. Diagonalization of the Hückel matrix results in closed shell, or “Hückel aromatic”, π-systems for benzene and Al$_4^{2-}$, and open shell, or “Hückel antiaromatic”, π-systems for cyclobutadiene and Al$_4^{4-}$, both in D_{4h} symmetry (see Figure 15).

Electron localization techniques such as Pipek−Mezey[129] or Foster−Boys,[131−133] as well as NBO analysis,[128] show that the σ-systems of the annulenes, including benzene and cyclobutadiene, can be easily localized, and each LMO can be assigned to a bond. However, the nonlocalizability of the σ-system in Al$_4^{n-}$ clusters using such procedures demonstrates the prevailing role of the σ-orbitals in the diamagnetic character of these metallic systems. Indeed, the current density maps of the six Pipek−Mezey localized σ-valence orbitals plotted by Fowler et al.[210] are intrinsically delocalized (see Figure 16).

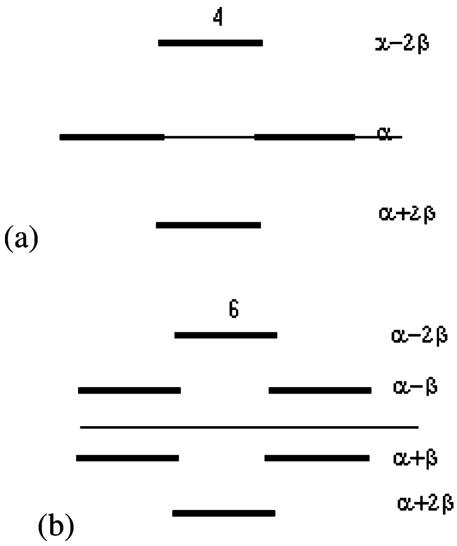

Figure 15. Hückel diagram for (a) D_{6h} and (b) D_{4h} annulenes. α denotes the diagonal, and β denotes the next neighbor elements of the Hückel Hamilton matrix.

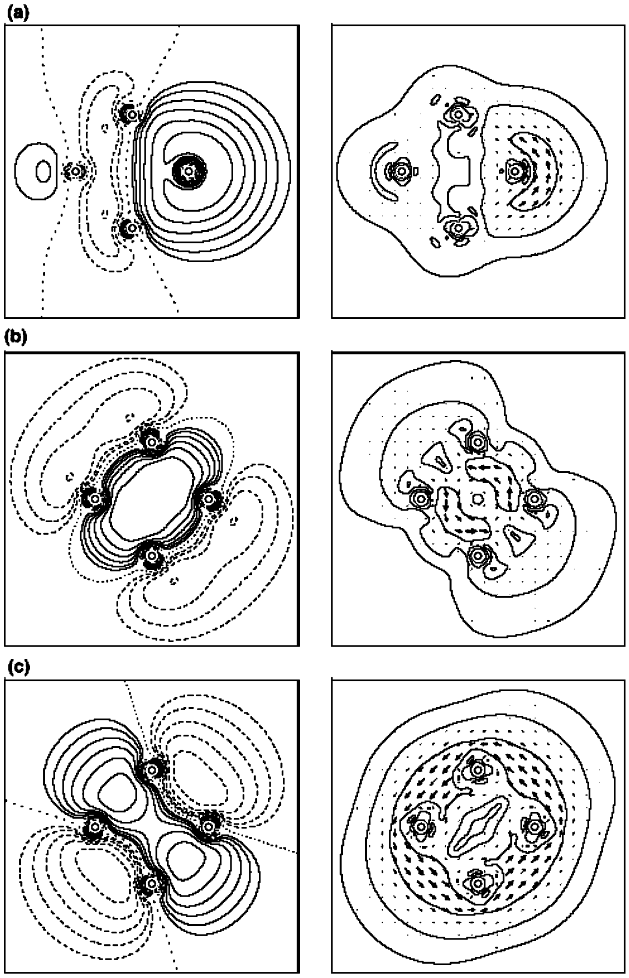

Figure 16. Localized σ-valence orbitals (left) and orbital current densities (right) in Al$_4^{2-}$: (a) one of the four equivalent lone pair hybrid orbitals produced by Pipek−Mezey localization, and (b and c) the cluster-bonding combinations produced by the same procedure. All maps are plotted in the molecular plane. Reprinted with permission from ref 210. Copyright 2002 Elsevier B. V.

Santos et al. have studied both the total and the $\sigma-\pi$ separated electron localization functions (ELF)[171,211,212] of these molecules.[213] They separated the total electron density into σ- and π−contributions and applied the ELF analysis independently to the total density as well as to the density arising from σ- and π-electrons. Furthermore, they quantified the degree of delocalization employing the bifurcation technique.[214] The points of bifurcation have been interpreted as a measure of the interaction among the different ELF basins and, chemically, as a measure of electron delocalization.[214,215] Looking at Figure 17, one can observe that the bifurcation value for the total ELF does not give a clear separation between the aromatic and the antiaromatic systems, whereas the bifurcation value for the ELF_π gives a clear separation. The aromatic rings present a high bifurcation value (0.91 for benzene), while the antiaromatic systems show rather small values (0.11 for the D_{2h} structure of cyclobutadiene). The D_{4h} Al_4^{2-} ion presents a surprisingly high ELF_π bifurcation value of 0.99, higher even than the value assigned to benzene. Note that this ion also presents a high bifurcation value for the ELF_σ ~0.88, which agrees with the prediction of a strong σ-delocalization in their four centers (which are nicely visualized in a plot of ELF_σ in Figure 3 of ref 213).

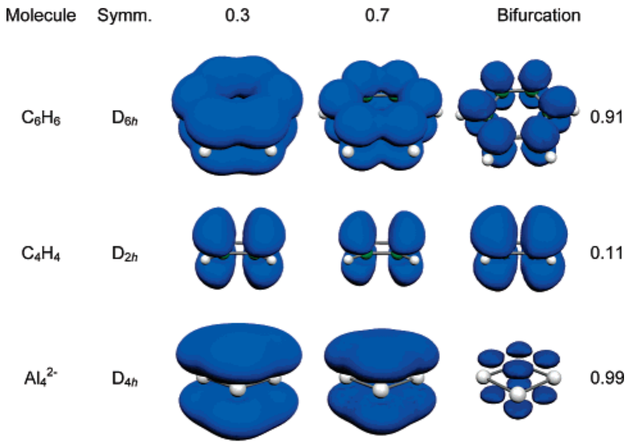

Figure 17. π-Localization domains for $\mathrm{ELF}_\pi = 0.3$, 0.7, and its respective bifurcation values. This figure has been kindly provided by Prof. P. Fuentealba.

Further evidence of the σ-delocalization in the D_{4h} Al_4^{2-} can be given by both the orbital contribution to the current density map and the analysis of the individual canonical molecular orbital (CMO) contributions to NICS (CMO-NICS), as described in more detail in the review of Chen et al.[105] Within gradient-corrected DFT, the six σ-orbitals contribute more than 50% of the diatropicity of D_{4h} Al_4^{2-},[216] while the sum of the CMO-NICS contributions of the σ−orbitals in both benzene and D_{2h} cyclobutadiene is positive (paratropic).[120] The Al_4^{2-} therefore benefits from both σ- and π-delocalization, thus justifying the stronger diatropic ring current (ARCS), benzene (9−12 nA T^{-1} for Al_4Li^- as compared to 8 nA T^{-1} for benzene).[191] In contrast, the magnetic character of annulenes is essentially determined by the property of the π-subsystem. Indeed, the overall diamagnetism of the benzene molecule is the result of cancellation of the effects of the paramagnetic circulation by the dominating diamagnetic contribution. The induced, first-order current density field for benzene in the molecular plane, obtained by Malagoli[84,98,217] using the CTOCD-DZ method (see Figure 18), clearly shows a paramagnetic circulation around the center of the ring due to the σ-electrons. In addition, while σ-electrons give rise to a diamagnetic local vortex close to the nucleus positions, the π-electrons are responsible for the diamagnetic circulations over the molecule as a whole, dominating the overall magnetic property of benzene.

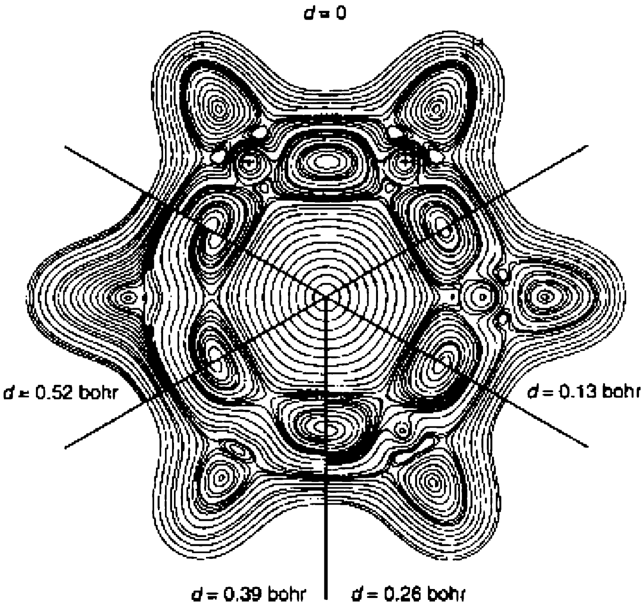

Figure 18. Projected diraction of the induced first-order, current density field for benzene, in the molecular plane ($d = 0$) and in planes parallel with it at distances of $d =$ 0.13, 0.26, 0.39, and 0.52 bohr with the CTOCD-DZ method. Reprinted with permission from an adaptation of refs 84, 98, and 217. Copyright 2000 Elsevier Science B. V.

Also, the torus-like topology of the ACID isosurface of benzene indicates a strong diamagnetic ring current.[178] Similar conclusions can be given using the very recent GIMIC method suggested by Jusélius, Sundholm, and Gauss.[86] The GIMIC method offers to integrate the current density along a cross-section, thus allowing a better classification of current densities, as pointed out by Jusélius, Sundholm, and Gauss: "Although the current density is a proper quantum mechanical observable, it has not been directly observed experimentally. As such, current density maps can convey information about molecules, thus aiding the understanding of the current paths in the molecule. However, current density plots do not provide any quantifiable measures of the current strengths nor are they suitable for comparing current strengths in different molecular systems. By integration over the current flow passing through specific bonds, it is possible to obtain the net current strengths around a molecular ring or through a bond."[86] Indeed, the integration of current densities in cross-sections can provide further information about the current flows in a molecule, as shown in Figure 19: In Figure 19a, the current density is

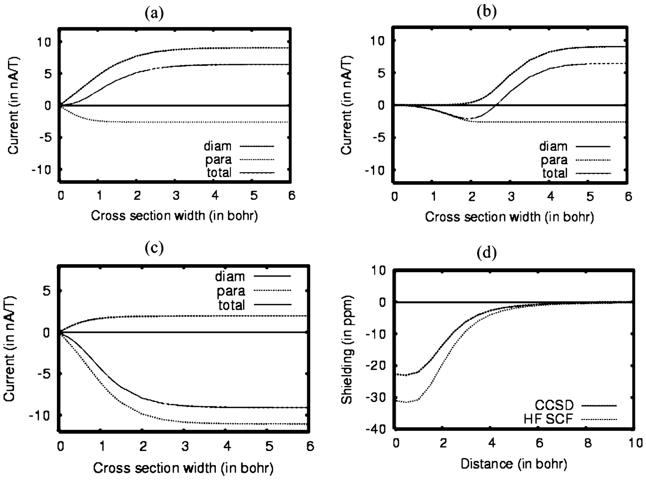

Figure 19. (a) Integrated current densities (GIMIC) of benzene with respect to the cross-section increasing perpendicular to the ring, (b) integrated GIMIC of benzene with cross-section chosen as diameter in the ring, (c) GIMIC of cylcobutadiene with cross-section perpendicular to the ring, and (d) comparison of the ARCS function for C_4H_4 at the HF and CCSD/TZP levels. These figures have been kindly provided by Dr. Dage Sundholm.

integrated along the z-axis, so perpendicular to the molecular plane, starting at the molecular plane ($z = 0$) until about $z = 3$ Å. The integrated current is diamagnetic and is saturated at about $z = 2$ Å. Within the GIMIC method, the paramagnetic current contribution is saturated earlier at $z = 1$ Å, indicating that it is dominated by the σ-framework. In Figure 19b, the current density is integrated along the radial distance from the ring center. The paramagnetic contributions arise close to the ring center, and the integrated current becomes diamagnetic after the current density has been integrated over the bonds.

In cyclobutadiene, the situation is reverse: Close to the molecular plane, a small diamagnetic current appears, while a much stronger paramagnetic current is induced and contributes for about 4 Å along the z-axis (Figure 19c). The GIMIC method can be employed together with high levels of theory, as, for example, with coupled cluster calculations, as shown in Figure 19d.

The prevalent role of the π-electrons in aromatic annulenes can also be evaluated in terms of their isotropic shieldings at the ring center (NICS_π). In these high-symmetry cases, the ring center coincides with the ring critical point of the electron density and the stagnation point of the current density. Indeed, both the GIAO (CMO-NICS_π)[120] and the LORG[59] techniques, applied with different underlying electron densities, give values larger than −20 ppm (−25.4 and −21.1 ppm, respectively) for benzene. In sharp contrast, the CMO-NICS_π of the paratropic D_{2h} cyclobutadiene is only +1.4 ppm.[120]

For nearly open shell systems such as C_4H_4 (i.e., for systems having a small HOMO−LUMO energy gap), NMR computations using perturbation theory suffer from numerical inaccuracies, and the level of theory might become important.[218] For instance, highly correlated methods such as CCSD/TZP give a smaller response than uncorrelated HF and hence smaller ring current as shown by comparing the ARCS function (eq 4.2) of C_4H_4 at different levels of theory (see Figure 19d).

The CMO-NICS values of the σ-system of Al_4^{4-} are found to be very similar to those of Al_4^{2-}, but the paratropic delocalization of the 4π-electrons partially overcomes the σ-diatropicity for Al_4^{4-}. However, unlike the Hückel antiaromatic cyclobutadiene, Al_4^{4-} still sustains a weak diatropic ring current.[159,191,216] These results further suggest that the π-electron counting rule used by Boldyrev and Wang[208] is misleading for predicting electronic delocalization in these molecules, in which the ring current effect cannot be solely attributed to the π-system (more details of this controversy can be found in *Chem. Eng. News* **2003**, *Dec 15*, 23).

Unlike in aromatic annulenes, the shielding in σ-aromatic molecules becomes paratropic at distances further from the center: The σ-ring current effects fall off away from rings much more rapidly than do π-effects. Although the ACID of Herges[178] has not yet been applied to σ-aromatic metal clusters, the illustration of the cyclic σ-type conjugation in cyclopropane using this method suggests that its application to these clusters may bring interesting insight. The Al_4^{n-} moieties have also been studied employing the GIMIC method to produce integrated current densities (Table 2). The method also allows one to subtract disturbing effects coming from the surrounding Li cations. The GIMIC method clearly shows that the Al_4^{2-} moiety is a diamagnetic molecule as no paramagnetic current is observed.

Table 2. GIMIC[86] Currents (nA/T) Above and Below the Ring at the CCSD/TZP Level

	Al_4Li^-	Al_4Li_2	$Al_4Li_3^-$	Al_4Li_4
diamagnetic current	30.5	36.7	18.4	17.1
paramagnetic current	0.0	0.0	−22.2	−20.5
total current	30.5	36.7	−3.8	−3.4
contribution from Li	5.5	11.0	−4.5	−6.5
total ring current	25.0	25.7	0.7	3.1

The total ring current is 25 ± 1 nA T^{-1} and is independent of the number of counterions used to stabilize the molecule. Even though numerical differences are larger for $Al_4Li_3^-$ and Al_4Li_4, these systems exhibit a strong paramagnetic current. This current is to some extent attributed to the Li ions, but most of it arises from the aluminum framework. The diamagnetic current is found to be only half of that of Al_4^{2-}, leading to a vanishing net total ring current for the Al_4^{4-} species.

Finally, the electron delocalization in these prototype systems is nicely illustrated by the plots of the IMF. As discussed in more detail in section 5, when applying an external magnetic field in the direction perpendicular to the molecular plane, antiaromatic annulenes such as C_4H_4 show a strong, long-ranged, paratropic response inside the ring. In contrast, the response inside the ring of the $4n + 2$ π-electron systems is purely diatropic. In Al_4^{2-}, the external magnetic field applied perpendicular to the ring also induces a long-ranged diatropic field inside the ring (Figure 20).[219] Indeed, the same magnetic response is observed for the IMF in both benzene and Al_4^{2-}. Although the IMF can convey information above the

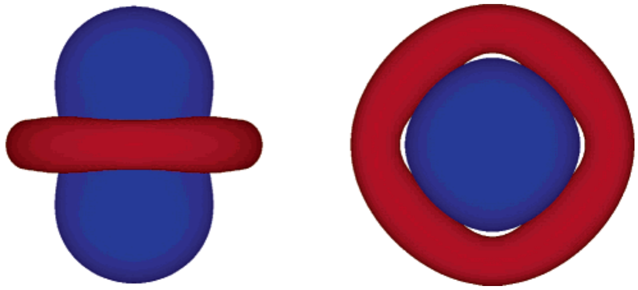

Figure 20. Isosurface of the z-component of the IMF $[(\vec{B}_{\mathrm{ind}})_z]$ at the PW91/IGLOIII level of theory. $(\vec{B}_{\mathrm{ind}})_z = 4$ μT and $(\vec{B}_{\mathrm{ext}})_z = B_{\mathrm{ext}} = 1$ T perpendicular to the magnetic plane, given in top and front views of the Al_4^{2-} molecule.

magnetic properties of molecules, it does not distinguish σ- from π-diatropic delocalization in Al_4^{2-}. Hence, the IMF analysis should be extended, and contributions arising from the decomposed shielding function, as done in dissected NICS, should be used to gain more information on the magnetic response of both σ- and π-systems.

7. Conclusions

In this review, special emphasis has been given to the computation of the magnetic shielding function associated to the response of a molecule toward an external magnetic field. It has been shown that the shielding function can be computed at any position in space and that the function is identical to the NMR chemical shielding tensors when calculated at the positions of the nuclei. In particular, the special properties of aromatic molecules induced by a magnetic perturbation have been discussed in terms of the magnetic shielding function, the ring current model, and the electron delocalization.

The qualitative analysis of aromatic character using the descriptors of current density or the tensorial magnetic shielding functions is rather insensitive to the computational method: The agreement between semiempirical, density functional-based and both, correlated and uncorrelated, ab initio methods is relatively good. Indeed, the way of treating the gauge problem, and perhaps problems with basis set convergence initiated due to an inefficient treatment of the gauge, affects the results usually more than the theoretical method itself.

The special role of electron delocalization of π-systems in carbon structures is discussed from the viewpoint of the establishment of semiempirical methods and in terms of various applications. In the fourth section, we discussed several models, which are related to the current density, namely, the mapping of the current density in several approaches, the topological analysis of the current density, the ACID approach, and the ARCS method. The fifth chapter was devoted to methods that are directly related with the computation of the magnetic shielding function in and around molecules. We have shown that a number of closely related approaches focus on the computation of the magnetic shielding function, either as a tensor or their isotropic value. As these approaches have been developed to suit different purposes, a unification of the terminology will be helpful for the general chemical community. The IMF can be computed directly from the shielding function and is also reviewed in section 5. Finally, in section 6, we compared the results of most of the methods discussed in this review on four illustrative molecules: the aromatic standard, benzene; the antiaromatic standard, D_{2h} cyclobutadiene; and the Al_4^{2-} and Al_4^{4-} clusters, which had led to controversial interpretations of aromaticity in the recent literature. In conclusion, each of the methods discussed in this article provides complementary insight and relevant information about the induced ring currents exhibited by these benchmark molecules. The interpretation of magnetic properties of a molecule may obviously vary when comparing different approaches. For instance, the current density maps, which display a vector field, only propose a qualitative view of the ring current. In contrast, the scalar fields provided by the NICS, the ACID, the IMF, or the GIMIC methods offer a quantitative view of the magnetic response. Also, the decomposition of any of these magnetic properties into its separated σ- and π-contributions provides a much more detailed insight as compared to the total electronic contribution.

8. Acknowledgments

We thank Dr. G. Merino for his clarifications on topological analysis and for preparation of Figure 3. Dr. D. Sundholm and Dr. J. Juselius are thanked for deep discussion on ARCS and GIMIC functions and for providing figures and prepublished information. We thank Dr. J. C. Santos and Prof. P. Fuentealba for the preparation of Figure 17. Prof. G. Grossmann is thanked for clarifying several problems concerning the graphical representation of shielding tensors. We thank Prof. P. v. R. Schleyer, Prof. R. B. King, and Prof. J. Weber for continuous support. Financial support by the Deutsche Forschungsgemeinschaft (DFG), the National Science Foundation Grant CHE-0209857, the University of Georgia, the Swiss National Foundation Grant 200020-100070, and the University of Geneva are gratefully acknowledged. This article is dedicated to Prof. Dr. Jacques Weber on his 65th birthday.

9. References

(1) Ramsey, N. F. *Phys. Rev.* **1950**, *78*, 699.
(2) *Calculation of NMR and EPR Parameters. Theory and Applications*; Kaupp, M., Bühl, M., Malkin, V. G., Eds.; Wiley-VCH: Weinheim, 2004.
(3) Lipscomb, W. N. *Adv. Magn. Res.* **1966**, *2*, 137.
(4) London, F. *J. Phys. Radium* **1937**, *8*, 397.
(5) Hameka, H. F. *Mol. Phys.* **1958**, *1*, 203.
(6) Pople, J. A. *Mol. Phys.* **1958**, *1*, 175.
(7) Ditchfield, R. *Mol. Phys.* **1974**, *27*, 789.
(8) Häser, M.; Ahlrichs, R.; Baron, H. P.; Weis, P.; Horn, H. *Theor. Chim. Acta* **1992**, *83*, 455.
(9) Wolinski, K.; Hinton, J. F.; Pulay, P. *J. Am. Chem. Soc.* **1990**, *112*, 8251.
(10) Pulay, P. *Modern Electronic Structure Theory*; World Scientific: Singapore, 1995.
(11) Pulay, P.; Hinton, J. F.; Wolinski, K. *Nuclear Magnetic Shieldings and Molecular Structure*; Kluwer: Boston, 1993.
(12) Jaszunski, M.; Szymanski, S.; Christiansen, O.; Jorgensen, P.; Helgaker, T.; Ruud, K. *Chem. Phys. Lett.* **1995**, *243*, 144.
(13) Ruud, K.; Helgaker, T.; Kobayashi, R.; Jorgensen, P.; Bak, K. L.; Jensen, H. J. A. *J. Chem. Phys.* **1994**, *100*, 8178.

(14) Gauss, J. *Ber. Bunsen-Ges.* **1995**, *99*, 1001.
(15) Fukui, H.; Baba, T.; Matsuda, H.; Miura, K. *J. Chem. Phys.* **1994**, *100*, 6608.
(16) Gauss, J.; Stanton, J. F. *J. Chem. Phys.* **1996**, *104*, 2574.
(17) Gauss, J.; Stanton, J. F. *Adv. Chem. Phys.* **2002**, *123*.
(18) Staemmler, V. Ruhr-Universität Bochum, 1978.
(19) Kutzelnigg, W. *Isr. J. Chem.* **1980**, *19*, 193.
(20) Schindler, M.; Kutzelnigg, W. *J. Chem. Phys.* **1982**, *76*, 1919.
(21) Schindler, M.; Kutzelnigg, W. *J. Am. Chem. Soc.* **1983**, *105*, 1360.
(22) Schindler, M.; Kutzelnigg, W. *Mol. Phys.* **1983**, *48*, 781.
(23) Hansen, A. E.; Bouman, T. D. *J. Chem. Phys.* **1985**, *82*, 5035.
(24) Keith, T. A.; Bader, R. F. W. *Chem. Phys. Lett.* **1992**, *194*, 1.
(25) Keith, T. A.; Bader, R. F. W. *Chem. Phys. Lett.* **1993**, *210*, 223.
(26) Lazzeretti, P.; Malagoli, M.; Zanasi, R. *Chem. Phys. Lett.* **1994**, *220*, 299.
(27) Hohenberg, P.; Kohn, W. *Phys. Rev. B* **1964**, *136*, B864.
(28) Kohn, W.; Sham, L. J. *Phys. Rev.* **1965**, *140*, 1133.
(29) Rajagopal, A. K.; Callaway, J. *Phys. Rev. B* **1973**, *7*, 1912.
(30) Rajagopal, A. K. *J. Phys. C* **1978**, *11*, L943.
(31) Eschrig, H.; Seifert, G.; Ziesche, P. *Solid State Commun.* **1985**, *56*, 777.
(32) Friedrich, K.; Grossmann, G.; Seifert, G. *Z. Chem.* **1988**, *28*, 156.
(33) Friedrich, K.; Seifert, G.; Grossmann, G. *Z. Phys. D: At. Mol. Clusters* **1990**, *17*, 45.
(34) Friedrich, K. Technische Universität Dresden, 1990.
(35) Bieger, W.; Seifert, G.; Eschrig, H.; Grossmann, G. *Chem. Phys. Lett.* **1985**, *115*, 275.
(36) Malkin, V. G.; Malkina, O. L.; Casida, M. E.; Salahub, D. R. *J. Am. Chem. Soc.* **1994**, *116*, 5898.
(37) Schreckenbach, G.; Ziegler, T. *J. Phys. Chem.* **1995**, *99*, 606.
(38) Bühl, M.; Kaupp, M.; Malkina, O. L.; Malkin, V. G. *J. Comput. Chem.* **1999**, *20*, 91.
(39) Schreckenbach, G.; Hay, P. J.; Martin, R. L. *J. Comput. Chem.* **1999**, *20*, 70.
(40) Salsbury, F. R.; Harris, R. A. *Chem. Phys. Lett.* **1997**, *279*, 247.
(41) Salsbury, F. R.; Harris, R. A. *J. Chem. Phys.* **1997**, *107*, 7350.
(42) Salsbury, F. R.; Harris, R. A. *J. Chem. Phys.* **1998**, *108*, 6102.
(43) Colwell, S. M.; Handy, N. C. *Chem. Phys. Lett.* **1994**, *217*, 271.
(44) Colwell, S. M.; Handy, N. C.; Lee, A. M. *Phys. Rev. A* **1996**, *53*, 1316.
(45) Harris, R. A.; Salsbury, F. R. *J. Chem. Phys.* **1998**, *109*, 2609.
(46) Lee, A. M.; Colwell, S. M.; Handy, N. C. *Chem. Phys. Lett.* **1994**, *229*, 225.
(47) Teale, A. M.; Tozer, D. J. *Chem. Phys. Lett.* **2004**, *383*, 109.
(48) Keal, T. W.; Tozer, D. J. *J. Chem. Phys.* **2003**, *119*, 3015.
(49) Wilson, P. J.; Tozer, D. J. *J. Mol. Struct. (THEOCHEM)* **2002**, *602*, 191.
(50) Ziegler, T. *Chem. Rev.* **1991**, *91*, 651.
(51) Slater, J. C. *Phys. Rev.* **1951**, *81*, 385.
(52) Malkin, V. G.; Malkina, O. L.; Erikson, L. A.; Salahub, D. R.; Politzer, P.; Seminario, J. M. *Modern Density Functional Theory: A Tool for Chemsitry*; Elsevier: Amsterdam, 1995.
(53) Malkin, V. G.; Malkina, O. L.; Salahub, D. R. *Chem. Phys. Lett.* **1993**, *204*, 80.
(54) Malkin, V. G.; Malkina, O. L.; Salahub, D. R. *Chem. Phys. Lett.* **1993**, *204*, 87.
(55) Cheeseman, J. R.; Trucks, G. W.; Keith, T. A.; Frisch, M. J. *J. Chem. Phys.* **1996**, *104*, 5497.
(56) Johnson, C. E.; Bovey, F. A. *J. Chem. Phys.* **1958**, *29*, 1012.
(57) Jameson, C. J.; Buckingham, A. D. *J. Phys. Chem.* **1979**, *83*, 3366.
(58) Jameson, C. J.; Buckingham, A. D. *J. Chem. Phys.* **1980**, *73*, 5684.
(59) Jensen, M. O.; Hansen, A. E. *Adv. Quantum Chem.* **1999**, *35*.
(60) Schleyer, P. V.; Maerker, C.; Dransfeld, A.; Jiao, H. J.; Hommes, N. J. R. V. *J. Am. Chem. Soc.* **1996**, *118*, 6317.
(61) Kaupp, M. In *Encyclopedia of Computational Chemistry*; Schleyer, P. v. R., Ed.; John Wiley and Sons: Chichester, 1998.
(62) Schleyer, P. V.; Jiao, H. J.; Hommes, N. J. R. V.; Malkin, V. G.; Malkina, O. L. *J. Am. Chem. Soc.* **1997**, *119*, 12669.
(63) Schleyer, P. V.; Manoharan, M.; Wang, Z. X.; Kiran, B.; Jiao, H. J.; Puchta, R.; Hommes, N. J. R. V. *Org. Lett.* **2001**, *3*, 2465.
(64) Chen, Z.; Heine, T.; Schleyer, P. v. R.; Sundholm, D. In *Calculation of NMR and EPR Parameters: Theory and Applications*; Kaupp, M., Bühl, M., Malkin, V. G., Eds.; Wiley-VCH: Weinheim, 2004.
(65) Wolinski, K. *J. Chem. Phys.* **1997**, *106*, 6061.
(66) Klod, S.; Kleinpeter, E. *J. Chem. Soc., Perkin Trans. 2* **2001**, 1893.
(67) Okninski, A.; Sadlej, A. J. *Acta Phys. Pol. A* **1975**, *48*, 455.
(68) Okninski, A.; Sadlej, A. J. *Acta Phys. Pol. A* **1975**, *48*, 435.
(69) Rossikhin, V. V.; Kuzmenko, V. V.; Voronkov, E. O.; Zaslavskaya, L. I. *J. Phys. Chem.* **1996**, *100*, 19801.
(70) Sadlej, A. J. *Mol. Phys.* **1973**, *26*, 1445.
(71) Bühl, M. In *Encyclopedia of Computational Chemistry*; Schleyer, P. v. R., Ed.; John Wiley and Sons: Chichester, 1998.
(72) Fleischer, U.; Kutzelnigg, W.; van Wüllen, C. In *Encyclopedia of Computational Chemistry*; Schleyer, P. v. R., Ed.; John Wiley and Sons: Chichester, 1998.
(73) Eschrig, H. *The Fundamentals of Density Functional Theory*; Teubner-Verlag: Leipzig, 2003.
(74) Hedin, L.; Lundqvist, B. I. *J. Phys. C* **1971**, *4*, 2064.
(75) Hückel, E. *Z. Elektrochem. Angew. Phys. Chem.* **1931**, *70*, 204.
(76) Hückel, E. *Z. Elektrochem. Angew. Phys. Chem.* **1931**, *72*, 310.
(77) Hückel, E. *Z. Elektrochem. Angew. Phys. Chem.* **1937**, *43*, 752.
(78) Pauling, L. *J. Chem. Phys.* **1936**, *4*, 673.
(79) Londsdale, K. *Proc. R. Soc. (London)* **1937**, *159*, 149.
(80) Pople, J. A. *J. Chem. Phys.* **1956**, *24*, 1111.
(81) Jackman, L. M.; Gaoni, Y.; Wolovsky, R.; Benefraim, D. A.; Bothnerby, A. A.; Sondheimer, F.; Amiel, Y. *J. Am. Chem. Soc.* **1962**, *84*, 4307.
(82) Keith, T. A. *Chem. Phys.* **1996**, *213*, 123.
(83) Keith, T. A.; Bader, R. F. W. *Can. J. Chem.* **1996**, *74*, 185.
(84) Lazzeretti, P. *Prog. Nucl. Magn. Reson. Spectrosc.* **2000**, *36*, 1.
(85) Zanasi, R.; Lazzeretti, P.; Malagoli, M.; Piccinini, F. *J. Chem. Phys.* **1995**, *102*, 7150.
(86) Juselius, J.; Sundholm, D.; Gauss, J. *J. Chem. Phys.* **2004**, *121*, 3952.
(87) Juselius, J.; Sundholm, D. *Phys. Chem. Chem. Phys.* **1999**, *1*, 3429.
(88) Schleyer, P. v. R. *Chem. Rev.* **2001**, *101*, 1115.
(89) Wannere, C. S.; Schleyer, P. V. *Org. Lett.* **2003**, *5*, 865.
(90) Wannere, C. S.; Sattelmeyer, K. W.; Schaefer, H. F.; Schleyer, P. V. R. *Angew. Chem., Int. Ed.* **2004**, *43*, 4200.
(91) Wannere, C. S.; Schleyer, P. V. R. *Org. Lett.* **2003**, *5*, 605.
(92) Viglione, R. G.; Zanasi, R.; Lazzeretti, P. *Org. Lett.* **2004**, *6*, 2265.
(93) Ferraro, M. B.; Lazzeretti, P.; Viglione, R. G.; Zanasi, R. *Chem. Phys. Lett.* **2004**, *390*, 268.
(94) Pelloni, S.; Ligabue, A.; Lazzeretti, P. *Org. Lett.* **2004**, *6*, 4451.
(95) Merino, G.; Heine, T.; Seifert, G. *Chem. Eur. J.* **2004**, *10*, 4367.
(96) Kleinpeter, E.; Klod, S. *J. Mol. Struct. (THEOCHEM)* **2004**, *704*, 79.
(97) Lazzeretti, P. *Phys. Chem. Chem. Phys.* **2004**, *6*, 217.
(98) Gomes, J.; Mallion, R. B. *Chem. Rev.* **2001**, *101*, 1349.
(99) Paquette, L. A.; Bauer, W.; Sivik, M. R.; Bühl, M.; Feigel, M.; Schleyer, P. V. *J. Am. Chem. Soc.* **1990**, *112*, 8776.
(100) Bühl, M.; Hommes, N.; Schleyer, P. V.; Fleischer, U.; Kutzelnigg, W. *J. Am. Chem. Soc.* **1991**, *113*, 2459.
(101) Bühl, M.; Thiel, W.; Jiao, H. J.; Schleyer, P. V.; Saunders, M.; Anet, F. A. L. *J. Am. Chem. Soc.* **1994**, *116*, 6005.
(102) Bühl, M.; Hirsch, A. *Chem. Rev.* **2001**, *101*, 1153.
(103) Williams, R. V.; Armantrout, J. R.; Twamley, B.; Mitchell, R. H.; Ward, T. R.; Bandyopadhyay, S. *J. Am. Chem. Soc.* **2002**, *124*, 13495.
(104) Van Lier, G.; Fowler, P. W.; De Proft, F.; Geerlings, P. *J. Phys. Chem. A* **2002**, *106*, 5128.
(105) Chen, Z. F.; Wannere, C. S.; Corminboeuf, C.; Schleyer, P. v. R. *Chem. Rev.* **2005**.
(106) Heilbronner, E.; Bock, H. *The HMO Model and Its Applications*; Wiley: London, 1976.
(107) Ivanov, V. K.; Kashenock, G. Y.; Polozkov, R. G.; Solov′yov, A. V. *J. Phys. B* **2001**, *34*, L669.
(108) Keller, S.; Engel, E. *Chem. Phys. Lett.* **1999**, *299*, 165.
(109) Yannouleas, C.; Landman, U. *Chem. Phys. Lett.* **1994**, *217*, 175.
(110) Albertazzi, E.; Domene, C.; Fowler, P. W.; Heine, T.; Seifert, G.; Van Alsenoy, C.; Zerbetto, F. *Phys. Chem. Chem. Phys.* **1999**, *1*, 2913.
(111) Warshel, A.; Karplus, M. *J. Am. Chem. Soc.* **1972**, *94*, 5612.
(112) Cornell, W. D.; Cieplak, P.; Bayly, C. I.; Gould, I. R.; Merz, K. M.; Ferguson, D. M.; Spellmeyer, D. C.; Fox, T.; Caldwell, J. W.; Kollman, P. A. *J. Am. Chem. Soc.* **1995**, *117*, 5179.
(113) Brenner, D. W. *Phys. Rev. B* **1992**, *46*, 1948.
(114) Brenner, D. W. *Phys. Rev. B* **1990**, *42*, 9458.
(115) Tersoff, J. *Phys. Rev. Lett.* **1988**, *61*, 2879.
(116) Seifert, G.; Porezag, D.; Frauenheim, T. *Int. J. Quantum Chem.* **1996**, *58*, 185.
(117) Porezag, D.; Frauenheim, T.; Kohler, T.; Seifert, G.; Kaschner, R. *Phys. Rev. B* **1995**, *51*, 12947.
(118) Fowler, P. W.; Heine, T.; Manolopoulos, D. E.; Mitchell, D.; Orlandi, G.; Schmidt, R.; Seifert, G.; Zerbetto, F. *J. Phys. Chem.* **1996**, *100*, 6984.
(119) Fowler, P. W.; Heine, T.; Mitchell, D.; Orlandi, G.; Schmidt, R.; Seifert, G.; Zerbetto, F. *J. Chem. Soc., Faraday Trans.* **1996**, *92*, 2203.
(120) Heine, T.; Schleyer, P. V.; Corminboeuf, C.; Seifert, G.; Reviakine, R.; Weber, J. *J. Phys. Chem. A* **2003**, *107*, 6470.
(121) Watson, M. A.; Salek, P.; Macak, P.; Helgaker, T. *J. Chem. Phys.* **2004**, *121*, 2915.
(122) Larsen, H.; Olsen, J.; Jorgensen, P.; Helgaker, T. *J. Chem. Phys.* **2001**, *115*, 9685.
(123) Helgaker, T.; Larsen, H.; Olsen, J.; Jorgensen, P. *Chem. Phys. Lett.* **2000**, *327*, 397.
(124) Scuseria, G. E. *J. Phys. Chem. A* **1999**, *103*, 4782.
(125) Scuseria, G. E.; Ayala, P. Y. *J. Chem. Phys.* **1999**, *111*, 8330.
(126) Ayala, P. Y.; Scuseria, G. E. *J. Chem. Phys.* **1999**, *110*, 3660.
(127) Burant, J. C.; Scuseria, G. E.; Frisch, M. J. *J. Chem. Phys.* **1996**, *105*, 8969.

(128) Bohmann, J. A.; Weinhold, F.; Farrar, T. C. *J. Chem. Phys.* **1997**, *107*, 1173.
(129) Pipek, J.; Mezey, P. G. *J. Chem. Phys.* **1989**, *90*, 4916.
(130) Fleischer, U.; Kutzelnigg, W.; Lazzeretti, P.; Muhlenkamp, V. *J. Am. Chem. Soc.* **1994**, *116*, 5298.
(131) Foster, J. M.; Boys, S. F. *Rev. Mod. Phys.* **1960**, *32*, 305.
(132) Foster, J. M.; Boys, S. F. *Rev. Mod. Phys.* **1960**, *32*, 303.
(133) Foster, J. M.; Boys, S. F. *Rev. Mod. Phys.* **1960**, *32*, 300.
(134) Choi, C. H.; Kertesz, M. *J. Chem. Phys.* **1998**, *108*, 6681.
(135) Pariser, R.; Parr, R. G. *J. Chem. Phys.* **1953**, *21*, 767.
(136) Pariser, R.; Parr, R. G. *J. Chem. Phys.* **1953**, *21*, 466.
(137) Pariser, R. *J. Chem. Phys.* **1953**, *21*, 568.
(138) Pople, J. A. *Trans. Faraday Soc.* **1953**, *49*, 1375.
(139) London, F. *J. Chem. Phys.* **1937**, *5*, 837.
(140) London, F. *C. R. Acad. Sci. (Paris)* **1937**, *28*, 205.
(141) Lazzeretti, P.; Zanasi, R. *J. Chem. Phys.* **1981**, *75*, 5019.
(142) Gomes, J. A. N. F. In *Local Density Approximations in Quantum Chemistry and Solid State Physics*; Dahl, J. P., Avery, J., Eds.; Plenum Press: New York, 1984.
(143) Gomes, J. *J. Chem. Phys.* **1983**, *78*, 4585.
(144) Gomes, J. *J. Mol. Struct. (THEOCHEM)* **1983**, *10*, 111.
(145) Gomes, J. A. N. F. *J. Chem. Phys.* **1983**, *78*, 3133.
(146) Gomes, J. *Mol. Phys.* **1982**, *47*, 1227.
(147) Keith, T. A.; Bader, R. F. W. *J. Chem. Phys.* **1993**, *99*, 3669.
(148) Coriani, S.; Lazzeretti, P.; Malagoli, M.; Zanasi, R. *Theor. Chim. Acta* **1994**, *89*, 181.
(149) Acocella, A.; Havenith, R. W. A.; Steiner, E.; Fowler, P. W.; Jenneskens, L. W. *Chem. Phys. Lett.* **2002**, *363*, 64.
(150) De Proft, F.; Fowler, P. W.; Havenith, R. W. A.; Schleyer, P. V. R.; Van Lier, G.; Geerlings, P. *Chem. Eur. J.* **2004**, *10*, 940.
(151) Fowler, P. W.; Steiner, E.; Zanasi, R.; Cadioli, B. *Mol. Phys.* **1999**, *96*, 1099.
(152) Fowler, P. W.; Steiner, E. *Chem. Phys. Lett.* **2002**, *364*, 259.
(153) Havenith, R. W. A.; Lugli, F.; Fowler, P. W.; Steiner, E. *J. Phys. Chem. A* **2002**, *106*, 5703.
(154) Havenith, R. W. A.; Rassat, A.; Fowler, P. W. *J. Chem. Soc., Perkin Trans. 2* **2002**, 723.
(155) Havenith, R. W. A.; Fowler, P. W.; Steiner, E. *Chem. Eur. J.* **2002**, *8*, 1068.
(156) Havenith, R. W. A.; Fowler, P. W.; Steiner, E. *Chem. Phys. Lett.* **2003**, *371*, 276.
(157) Havenith, R. W. A.; Fowler, P. W.; Jenneskens, L. W.; Steiner, E. *J. Phys. Chem. A* **2003**, *107*, 1867.
(158) Havenith, R. W. A.; Jenneskens, L. W.; Fowler, P. W. *Chem. Phys. Lett.* **2003**, *367*, 468.
(159) Havenith, R. W. A.; Fowler, P. W.; Steiner, E.; Shetty, S.; Kanhere, D.; Pal, S. *Phys. Chem. Chem. Phys.* **2004**, *6*, 285.
(160) Havenith, R. W. A.; Engelberts, J. J.; Fowler, P. W.; Steiner, E.; van Lenthe, J. H.; Lazzeretti, P. *Phys. Chem. Chem. Phys.* **2004**, *6*, 289.
(161) Steiner, E.; Fowler, P. W. *J. Phys. Chem. A* **2001**, *105*, 9553.
(162) Steiner, E.; Fowler, P. W.; Havenith, R. W. A. *J. Phys. Chem. A* **2002**, *106*, 7048.
(163) Steiner, E.; Fowler, P. W.; Viglione, R. G.; Zanasi, R. *Chem. Phys. Lett.* **2002**, *355*, 471.
(164) Steiner, E.; Fowler, P. W. *Org. Biomol. Chem.* **2003**, *1*, 1785.
(165) Zanasi, R. *J. Chem. Phys.* **1996**, *105*, 1460.
(166) Fowler, P. W.; Zanasi, R.; Cadioli, B.; Steiner, E. *Chem. Phys. Lett.* **1996**, *251*, 132.
(167) Ceulemans, A.; Beyens, D.; Vanquickenborne, L. G. *J. Am. Chem. Soc.* **1984**, *106*, 5824.
(168) Murrayrust, P.; Burgi, H. B.; Dunitz, J. D. *Acta Crystallogr. A* **1979**, *35*, 703.
(169) Stevens, R. M.; Lipscomb, W. N.; Pitzer, R. M. *J. Chem. Phys.* **1963**, *38*, 550.
(170) Gomes, J. *Phys. Rev. A* **1983**, *28*, 559.
(171) Merino, G.; Vela, A. V.; Heine, T. *Chem. Rev.* **2005**, *105*, 3812.
(172) Bader, R. F. W. *Int. J. Quantum Chem.* **1994**, *49*, 299.
(173) Bader, R. F. W.; Matta, C. F. *J. Phys. Chem. A* **2004**, *108*, 8385.
(174) Bader, R. F. W.; Zou, P. F. *Chem. Phys. Lett.* **1992**, *191*, 54.
(175) Bader, R. F. W.; Keith, T. A.; Gough, K. M.; Laidig, K. E. *Mol. Phys.* **1992**, *75*, 1167.
(176) Bader, R. F. W. *Theor. Chem. Acc.* **2001**, *105*, 276.
(177) Bader, R. F. W.; Keith, T. A. *J. Chem. Phys.* **1993**, *99*, 3683.
(178) Herges, R.; Geuenich, D. *J. Phys. Chem. A* **2001**, *105*, 3214.
(179) Herges, R.; Papafilippopoulos, A. *Angew. Chem., Int. Ed.* **2001**, *40*, 4671.
(180) Kimball, D. B.; Weakley, T. J. R.; Herges, R.; Haley, M. M. *J. Am. Chem. Soc.* **2002**, *124*, 13463.
(181) Montero-Campillo, M. M.; Rodriguez-Otero, J.; Cabaleiro-Lago, E. M. *J. Phys. Chem. A* **2004**, *108*, 8373.
(182) Rodriguez-Otero, J.; Cabaleiro-Lago, E. M.; Hermida-Ramon, J. M.; Pena-Gallego, A. *J. Org. Chem.* **2003**, *68*, 8823.
(183) Marsella, M. J.; Yoon, K.; Almutairi, A.; Butt, S. K.; Tham, F. S. *J. Am. Chem. Soc.* **2003**, *125*, 13928.
(184) Herges, R. *Chem. Rev.* **2005**, *105*, 3758.
(185) Ligabue, A.; Sauer, S. P. A.; Lazzeretti, P. *J. Chem. Phys.* **2003**, *118*, 6830.
(186) Johansson, M. P.; Juselius, J.; Sundholm, D. *Angew. Chem., Int. Ed.* **2005**, *44*, 1843.
(187) Juselius, J.; Patzschke, M.; Sundholm, D. *J. Mol. Struct. (THEOCHEM)* **2003**, *633*, 123.
(188) Corminboeuf, C.; Heine, T.; Weber, J. *Phys. Chem. Chem. Phys.* **2003**, *5*, 246.
(189) Juselius, J.; Sundholm, D. *J. Org. Chem.* **2000**, *65*, 5233.
(190) Juselius, J.; Sundholm, D. *Phys. Chem. Chem. Phys.* **2000**, *2*, 2145.
(191) Juselius, J.; Straka, M.; Sundholm, D. *J. Phys. Chem. B* **2001**, *105*, 24A.
(192) Jensen, M. O.; Thorsteinsson, T.; Hansen, A. E. *Int. J. Quantum Chem.* **2002**, *90*, 616.
(193) Bilde, M.; Hansen, A. E. *Mol. Phys.* **1997**, *92*, 237.
(194) Hansen, A. E.; Bilde, M. In *Encyclopedia of Nuclear Magnetic Resonance*; Grant, D. M., Harris, R. K., Eds.; John Wiley and Sons: Chichester, 1996; Vol. 7.
(195) Hansen, A. E.; Bouman, T. D. In *Nuclear Magnetic Shielding and Molecular Structure*; Tossell, J. A., Ed.; Kluwer: Dordrect, 1993.
(196) Hansen, A. E.; Mikkelsen, K. V.; Bak, K. L. *Magn. Reson. Rev.* **1997**, *17*, 133.
(197) Hansen, A. E.; Bouman, T. D. *J. Chem. Phys.* **1989**, *91*, 3552.
(198) Radeglia, R. *Solid State Nucl. Magn. Res.* **1995**, *4*, 317.
(199) Trahanovsky, W. S.; Fischer, D. R. *J. Am. Chem. Soc.* **1990**, *112*, 4971.
(200) Roberts, J. D.; Streitwieser, A.; Regan, C. M. *J. Am. Chem. Soc.* **1952**, *74*, 4579.
(201) Karadakov, P. B.; Gerratt, J.; Cooper, D. L.; Raimondi, M.; Sironi, M. *Int. J. Quantum Chem.* **1996**, *60*, 545.
(202) Benassi, R.; Ianelli, S.; Nardelli, M.; Taddei, F. *J. Chem. Soc., Perkin Trans. 2* **1991**, 1381.
(203) Faust, R.; Glendening, E. D.; Streitwieser, A.; Vollhardt, K. P. C. *J. Am. Chem. Soc.* **1992**, *114*, 8263.
(204) McKee, M. L.; Balci, M.; Kilic, H.; Yurtsever, E. *J. Phys. Chem. A* **1998**, *102*, 2351.
(205) Klod, S.; Koch, A.; Kleinpeter, E. *J. Chem. Soc., Perkin Trans. 2* **2002**, 1506.
(206) Günther, H. *NMR Spectroscopy: Basic Principles, Concepts, and Applications in Chemistry*, 2nd ed.; Wiley: Chichester; New York, 1995.
(207) Merino, G.; Mendez-Rojas, M. A.; Beltraan, H. I.; Corminboeuf, C.; Heine, T.; Vela, A. *J. Am. Chem. Soc.* **2004**, *126*, 16160.
(208) Kuznetsov, A. E.; Birch, K. A.; Boldyrev, A. I.; Li, X.; Zhai, H. J.; Wang, L. S. *Science* **2003**, *300*, 622.
(209) Li, X.; Kuznetsov, A. E.; Zhang, H. F.; Boldyrev, A. I.; Wang, L. S. *Science* **2001**, *291*, 859.
(210) Fowler, P. W.; Havenith, R. W. A.; Steiner, E. *Chem. Phys. Lett.* **2002**, *359*, 530.
(211) Becke, A. D.; Edgecombe, K. E. *J. Chem. Phys.* **1990**, *92*, 5397.
(212) Sola, M.; Silvi, B. *Chem. Rev.* **2005**, *105*, 3911.
(213) Santos, J. C.; Tiznado, W.; Contreras, R.; Fuentealba, P. *J. Chem. Phys.* **2004**, *120*, 1670.
(214) Savin, A.; Silvi, B.; Colonna, F. *Can. J. Chem.* **1996**, *74*, 1088.
(215) Savin, A.; Nesper, R.; Wengert, S.; Fassler, T. F. *Angew. Chem. Int. Ed.* **1997**, *36*, 1809.
(216) Chen, Z. F.; Corminboeuf, C.; Heine, T.; Bohmann, J.; Schleyer, P. V. *J. Am. Chem. Soc.* **2003**, *125*, 13930.
(217) Malagoli, M. Ph.D. Thesis, University of Modena, Modena, 1993.
(218) Van Wüllen, C.; Kutzelnigg, W. *Chem. Phys. Lett.* **1993**, *205*, 563.
(219) Merino, G.; Heine, T. Manuscript in preparation.

CR030082K